miR-126 binds to the 3'UTR of EGFL7

Emilía Sif Ásgrímsdóttir

Faculty of Life and Environmental Sciences
School of Engineering and Natural Sciences
University of Iceland
2015

miR-126 binds to the 3'UTR of EGFL7

Emilía Sif Ásgrímsdóttir

14 ECTS thesis submitted in partial fullfillment of a
Baccalaureus Scientiarum degree in Molecular Biology

Advisors
Guðrún Valdimarsdóttir
Anne Richter

Faculty of Life and Environmental Sciences
School of Engineering and Natural Sciences
University of Iceland
Reykjavík, May 2015

miR-126 binds to the 3'UTR of EGFL7
14 ECTS thesis submitted in partial fullfillment of a *Baccalaureus Scientiarum* degree in Biochemistry and Molecular Biology

Faculty of Life and Environmental Sciences
School of Engineering and Natural Sciences
University of Iceland
Askja, Sturlugata 7
101 Reykjavík
Telephone: 525 4000

Bibliographic information:
Emilía Sif Ásgrímsdóttir, 2015, *miR-126 binds to the 3'UTR of EGFL7*, B.Sc thesis, Faculty of Life and Environmental Sciences, Univeristy of Iceland, 29 pages.

Print: Háskólaprent ehf.
Reykjavík, May 2015

Útdráttur

Þroskun æðaþels er mikilvægt ferli til að mynda nýjar æðar, bæði í fósturþroska og á seinni stigum ævinnar. Æðakerfi líkamans mótast í fósturþroska og á síðari stigum vaxa nýjar æðar út frá þessu æðakerfi, svo sem í sáraviðgerðum og framvindu krabbameins. Þroskun æðaþels er vandlega stjórnað af mörgum þáttum og ferlum sem vinna saman til að móta flókið æðakerfi líkamans. Rannsóknir á þeim þáttum sem hafa áhrif á þroskun æðaþels og hvernig þeir vinna saman veita bæði innsýn í grundvallar þroskunarferli æðamyndunar og möguleika á því að síðar verði hægt að nota þessa þekkingu til lækninga á sjúkdómum. Til dæmis er framvinda krabbameins og meinvörpun háð því að nýjar æðar vaxi til æxlisins og stjórnun á þessu ferli gæti nýst til krabbameinsmeðferðar.

Rannsóknarhópur Guðrúnar Valdimarsdóttur hefur unnið að því að rannsaka tengingu á milli BMP-Smad1/5 boðleiðarinnar, EGFL7 og miR-126 í þroskun æðaþels. Í þessu verkefni var leitast við að rannsaka hvort að miR-126 gæti bundist 3'UTR svæði genanna EGFL7, TMEM100 og Smad6 og þar með sýna fram á tengingu milli BMP-Smad1/5 boðleiðarinnar, EGFL7 og miR-126. Í þeim tilgangi voru búnar til genaferjur sem innihéldu klöguskjóðugen fyrir framan 3'UTR svæði genanna EGFL7, TMEM100 og Smad6. Genaferjunum var svo skeytt inn í HEK frumur sem yfirtjáðu miR-126 og binding miR-126 við 3'UTR svæðin var metin út frá virkni klöguskjóðunnar. Niðurstöður þessarar rannsóknar veita vísbendingu um að miR-126 bindi 3'UTR svæði genanna EGFL7 og Smad6 en bindi ekki 3'UTR svæði gensins TMEM100.

Abstract

Endothelial development is an important process for generating new blood vessels during embryonic development as well as in the adult life. During embryogenesis, the endothelial network is established and this network is then remodeled in wound repair and cancer progression, e.g. Development of the endothelium is a closely controlled process, regulated by many different factors and pathways that work together to form the complex endothelial network. By identifying these factors and the interplay between them we not only shed light on this fundamental developmental process but also open possibilities that this knowledge could be used for therapeutic purposes. Most notably, the progression of cancer and metastasis is dependent on the development of new blood vessels and controlling this process could be vital in cancer treatments.

Preliminary studies of the research group have suggested a connection between the BMP-Smad1/5 signaling pathway, EGFL7 and miR-126 in endothelial development. The aim of this project was to determine whether miR-126 could bind to the 3'UTR sequences of EGFL7, TMEM100 and Smad6 and therefore demonstrate a connection between BMP-Smad1/5 signaling pathway, EGFL7 and miR-126. For this purpose we created a pISO reporter plasmid that contained the 3'UTR sequences of EGFL7, TMEM100 and Smad6, respectively, behind a luciferase reporter gene. HEK cells that overexpressed miR-126 were then transfected with the reporter plasmids and binding was assessed according to luciferase activity. The results of this study provide evidence that miR-126 does bind to the 3'UTR sequences of EGFL7 and Smad6 but does not bind to the 3'UTR sequence of TMEM100.

Table of contents

Figures

Tables

Abbreviations

3'UTR	3' Untranslated Region
AGO	Argonaute proteins
ALK	Activin Repector-like Kinase
BMP	Bone Morphogenetic Protein
Dll4	Delta-like Protein 4
ECM	Extracellular matrix
EGF	Epidermal Growth Factor
EGFL7	Epidermal Growth Factor-Like Domain 7
eIF	Eukaryotic Initation Factor
FGF2	Fibroblast Growth Factor 2
HEK	Human Embryonic Kidney
hESC's	Human Embryonic Stem Cells
MAP	Mitogen Activated Protein
MEF	Mouse Embryonic Fibroblasts
miR-126	microRNA-126
miRNA	microRNA
mRNA	messenger RNA
NICD	Notch Intracellular Domain
PBS	Phosphate Buffered Saline
PCR	Polymerase Chain Reaction
PI3	Phospoinositide-3-Kinase
PIK3R2	Phospoinositide-3-Kinase Regulatory Subunit 2
RISC	RNA-Induced Silencing Complex
SPRED1	Sprouty-related EVH1 domain-containing protein 1
TGFβ	Transforming Growth Factor β
TMEM100	Transmembrane Protein 100
VEGF	Vascular Endothelial Growth Factor

Acknowledgements

First and foremost I would like to thank my supervisor, Guðrún Valdimarsdóttir, for giving me the great opportunity to study under her supervision.

I would also like to give thanks to my instructor, Anne Richter, for her endless patience and all her help with this project.

Finally, I would like to thank my family and friends for all their support and especially my mother and aunt for proof reading this paper.

1 Introduction

1.1 Stem Cells

Stem cells can be defined as unspecialized cells that have the unique ability to either continuously self-renew or differentiate into various specialized cell types (Ratajczak et al. 2008). These unique cells play a crucial role in embryonic development but their use is not restricted to the early stages of life. Stem cells are also responsible for the regeneration of tissue during adult life. The differentiated tissue of numerous mature organs retains subpopulations of relatively undifferentiated adult stem cells that can give rise to a limited set of cell types (Lemoli et al., 2005).

Stem cells can divide asymmetrically or symmetrically. Asymmetric division generates one new stem cell and a daughter cell that is more developmentally committed. This type of division has long been thought to be a defining characteristic of stem cells. In contrast, symmetric division produces either two daughter stem cells or two more differentiated progeny. During symmetric division some cells are more prone to divide into new stem cells and others into differentiated cells. This type of division has an advantage when the stem cell pool needs to be replenished e.g. in response to injury (Shahriyari & Komarova 2013).

Potency is the ability of a stem cell to generate various different types of specialized cells. Stem cells can be classified into four groups according to potency. The most potent stem cells of an organism are the *totipotent* cells. The zygote is a totipotent cell and it is able to give rise to every cell in the embryo as well as the trophoblast cells of the placenta. During embryonic development stem cells lose their totipotency and become *pluripotent*. Pluripotent cells are found in the inner cell mass of the blastocyst and have the ability to form all three germ layers of the embryo; the endoderm, ectoderm and mesoderm (Ratajczak et al. 2008). *Multipotent* stem cells are found in both the embryo and the adult. They are partially committed to a subset of cell types and can only generate cells from one of the three germ layers. *Unipotent* stem cells are fully committed to the particular tissue they reside in and can only regenerate one specific type of cell (Gilbert, 2014).

Embryonic stem cells (ESCs) are pluripotent stem cells that are isolated from the inner cell mass of the blastocyst. When ESCs are grown in culture they maintain their pluripotent state and have the capacity for infinite self-renewal and the ability to differentiate into all somatic cell types (Figure 1). Because of their unique nature, ESCs hold an enormous promise as tools for understanding normal development and disease (Puri & Nagy 2012).

1.1.1 Stem cell differentiation

The environment largely determines the fate of a stem cell. Stem cell niches are regulating microenvironments composed of a population of specialized cells that maintain proliferation and differentiation of the stem cells via paracrine or juxtacrine factors (Yin & Li 2006). When stem cells leave the niche these factors can no longer reach them and the cells begin differentiating in response to the cells and the extracellular matrix that make up their new environment (Burdick & Vunjak-Novakovic 2009).

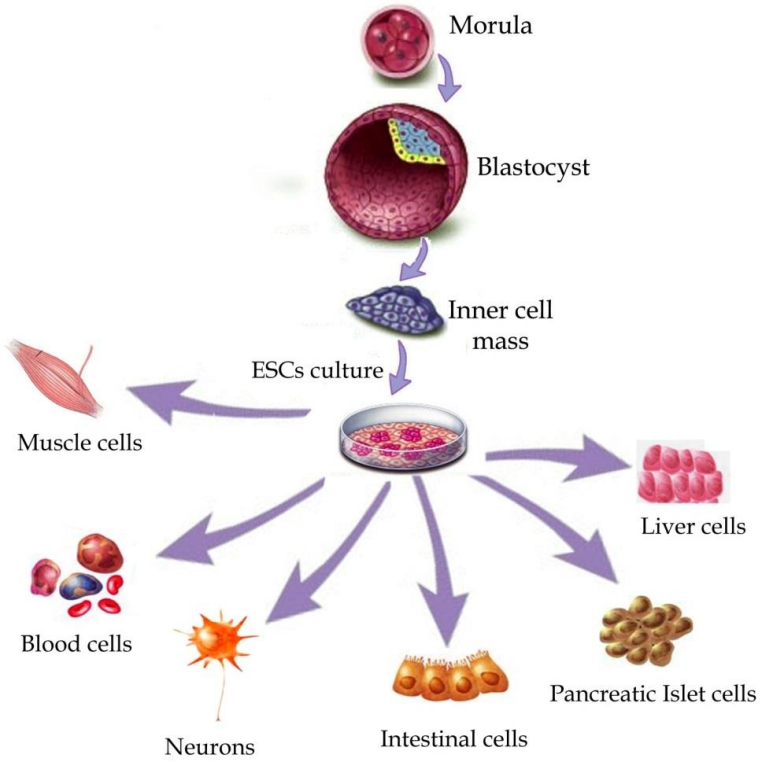

Figure 1. **Embryonic stem cell differentiation.** Embryonic stem cells are isolated from the inner cell mass of the blastocyst. They are pluripotent and can therefore both self-renew and differentiate into all cell types of the body (Mirella Meregalli 2011).

Controlling stem cell differentiation in the laboratory can prove to be difficult because the complex process of differentiation *in vivo* is not easily mimicked in culture (Burdick & Vunjak-Novakovic 2009). There are two main methods for differentiation *in vitro*: spontaneous and directed. Spontaneous and random differentiation can easily be triggered if the stem cells are allowed to aggregate into embryoid bodies. This leads to the formation of structures that can yield cells of the three germ layers (Heo et al. 2005). Directed differentiation is more challenging. It is possible to encourage the stem cells to differentiate into a particular cell type by using specific growth factors in the medium, growing the cells in co-culture with specialized cells or by manipulating certain cellular pathways. However, perfect control of differentiation is not yet possible and the final culture always contains a mixture of various cell types (Passier & Mummery 2003).

1.2 Mesodermal development

During early embryonic development the three germ layers are formed. The three germ layers are the endoderm, ectoderm and mesoderm, and together they will form all the organs of the embryo. The mesoderm is divided into the paraxial, intermediate and lateral plate mesoderm, depending on which organ it will form during development (Doss et al. 2012). The lateral plate mesoderm will give rise to the circulatory system during vasculogenesis (*Developmental Biology, Tenth Edition*, 2014).

1.2.1 Vasculogenesis

The vascular network is one of the first organs formed in the early embryo (Velazquez 2007). Vasculogenesis is split into two distinct phases: first the angioblasts differentiate from mesodermal cells and then the angioblasts form primitive blood vessels (Risau & Flamme

1995). In the first phase of vasculogenesis, mesodermal cells leaving the primitive streak become hemangioblasts, the precursors of both the blood cells and blood vessels (*Developmental Biology, Tenth Edition*, 2014). The hemangioblasts then condense into blood islands in the yolk sac and differentiate into hematopoetic cells and angioblasts (Velazquez 2007). In the second phase of vasculogenesis, primitive blood vessels are formed. The angioblasts proliferate and differentiate into endothelial cells, the inner lining of blood vessels. The endothelial cells then form tubes and connect to form a capillary network (*Developmental Biology, Tenth Edition*, 2014). Two growth factors are absolutely necessary to initiate vasculogenesis, the basic fibroblast growth factor 2 (FGF2) and the vascular endothelial growth factor (VEGF) family. FGF2 is required for the formation of hemangioblasts from mesodermal cells and the VEGF family promotes angioblast proliferation and differentiation into endothelial cells, as well as tube formation (Carmeliet & Jain 2011). Even though FGF2 and VEGF are the most known factors critically responsible for initiating vasculogenesis many other factors affect endothelial cell fate. For instance, the family of bone morphogenetic proteins (BMPs) of the transforming growth factor-β (TGF-β) superfamily has been shown to stimulate vasculogenesis through gain and loss of function models. Additionally, BMPs interact with pathways involved in vasculogenesis, such as VEGF signaling (Moser & Patterson 2005) .

1.2.2 Angiogenesis

Whereas vasculogenesis is the *de novo* formation of blood vessels from mesodermal precursors, angiogenesis is the generation of new blood vessels through remodeling of the existing capillary network (Drake 2003). During angiogenesis, angiogenic factors activate endothelial cells. In response, cell-cell junctions between the endothelial cells and the basal membrane are re-modeled to accommodate the migration of the endothelial cells. This process is termed sprouting and it is characterized by two types of cells; tip cells and stalk cells. Tip cells will migrate in response to a gradient of sprouting inducers and the sprout is elongated through proliferation of the stalk cells. When tip cells from neighboring sprouts meet, they connect to form a new branch of the capillary network (Welti et al. 2013). Numerous inducers of angiogenesis have been identified, for example members of the vascular endothelial growth factor (VEGF), transforming growth factor beta (TGFβ) and epidermal growth factor (EGF) families (Otrock et al. 2007; Goumans et al. 2002; van Cruijsen et al. 2005).

1.3 microRNA

microRNAs (miRNAs) constitute a large family of small, non-coding RNAs that are approximately 21 nucleotides long. miRNAs were first discovered over 20 years ago and since then, they have emerged as key post-transcriptional regulators of gene expression in both animals, plants and protozoa. In mammals, miRNAs appear to regulate the activity of about 60% of protein-coding genes and they take part in the regulation of most cellular processes investigated thus far (Fabian et al. 2010). Furthermore, changes in miRNA expression have been linked to various human pathologies, such as cancer (Filipowicz et al. 2008).

Mature miRNAs are processed from double-stranded RNA precursors called pri-miRNAs. These precursors fold into a hairpin structure with imperfect base pairing and are then exported out of the nucleus for processing, catalyzed by the enzymes Drosha and Dicer. pri-miRNAs are processed into ~70 nucleotide hairpins called pre-miRNAs. Finally, the

pre-miRNAs are cleaved by Dicer resulting in ~21 nucleotide miRNA duplexes with protruding 3' ends. One strand is then chosen to function as a mature miRNA and the other is degraded (Du & Zamore 2005). miRNAs function as a part of a complex, referred to as the RNA-induced silencing complex (RISC). RISC is composed of multiple proteins but the most important and well defined components of RISC are the proteins of the Argonaute (AGO) family (Sontheimer 2005).

1.3.1 microRNAs regulate gene expression

microRNAs regulate gene expression post-transcriptionally, either by repressing the translation of messenger RNAs (mRNAs) into proteins or by destabilizing mRNAs in the cytoplasm (Fabian et al. 2010). miRNAs exert their function by various methods. In plants, miRNAs tend to base pair with their target sequences with near perfect complementarity to cause endonucleolytic cleavage of the mRNA molecules (Jones-Rhoades et al. 2006). Animals such as vertebrates utilize this mechanism in some instances, but other methods detailed in this chapter are more common. Generally, the miRNAs imperfectly base pair with their target sequences, which are usually located in the 3'UTR sequence of the mRNA molecule. The most rigid requirement is that a six-nucleotide sequence on the miRNA called the seed region is perfectly and continuously base paired. Mismatches in the seed region greatly affect repression (Brennecke et al. 2005).

As previously mentioned, miRNAs have been shown to regulate gene expression by repressing protein translation. However, whether this repression occurs at the initiation, elongation or termination step of translation remains unclear. Initiation is the most complex step, providing the most opportunities for intervention. During initiation, the eIF translation initiation factor recognizes and binds to the 5'-terminal mRNA cap and this leads to the assembly of the ribosome. Research has shown that the AGO proteins in RISC have sequence homology to the cap-binding region of the eIF factor and could compete with eIF to bind the 5'-terminal cap. The AGO proteins could therefore hinder the assembly of the ribosome (Filipowicz et al. 2008). However, it is unlikely that miRNAs exclusively repress protein translation at the initiation step. Various studies have indicated that miRNAs can also affect post initiation steps. Some mRNAs remain associated with ribosomes even though the amount of their protein products is greatly reduced and several miRNAs and AGO proteins have also been shown to associate with ribosomes. This seems to indicate that miRNAs do not hinder the assembly of the ribosome but instead somehow affect the elongation step of translation (Fabian et al. 2010).

The second method of gene expression regulation mediated by miRNAs involves destabilization of mRNA molecules in the cytoplasm. Early research indicated that miRNA regulation of protein synthesis did not involve changes in mRNA levels but recent research has shown that repression of many mRNA targets is associated with destabilization and subsequent degradation of the mRNA molecules (Wu et al. 2006). In eukaryotes, mRNA is degraded by two pathways, both of which involve initial shortening of the mRNA poly(A) tail. After poly(A) shortening, the remaining mRNA can then either be degraded by the exosome or by removal of the mRNA cap catalyzed by the exonuclease XRN1. miRNAs can therefore control levels of mRNA by recruiting components of the degradation machinery leading to poly(A) shortening, de-capping and subsequent degradation (Filipowicz et al. 2008).

1.4 EGFL7 and miR-126 in vascular development

Vasculogenesis is a complex process that is finely regulated by a vast array of different factors. Identification of these factors has been a prime focus of cardiovascular research for many years. Epidermal Growth Factor-Like Domain 7 (EGFL7) is a newly discovered angiogenic signaling factor. Research has demonstrated that EGFL7 is important both in vasculo- and angiogenesis but its precise role during vascular development has not been fully established (Parker et al. 2004). The EGFL7 gene is located on the human chromosome 9 and it encodes a 30 kDA protein which is highly conserved among vertebrates (Nichol & Stuhlmann 2012). The biologically active miRNA miR-126 is located within intron 7 of the EGFL7 gene (Figure 2).

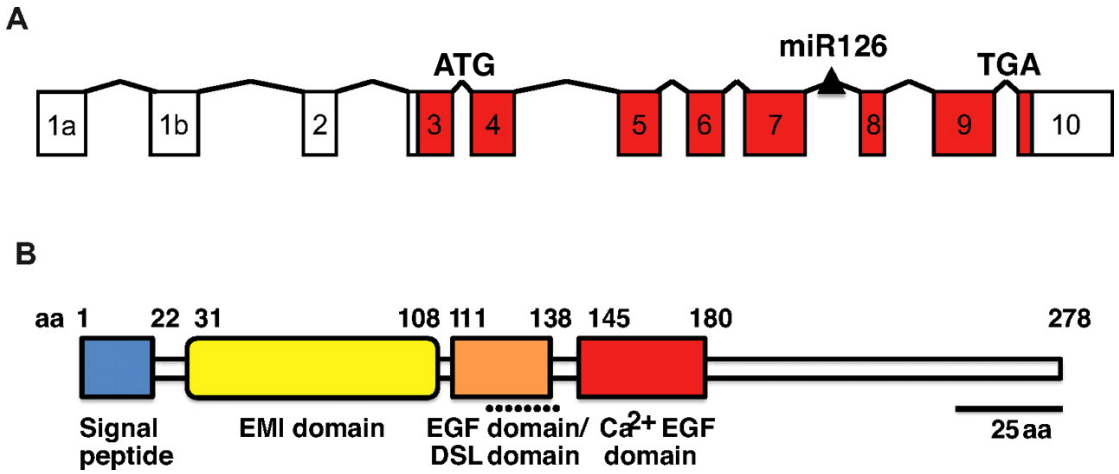

Figure 2. Gene and protein structure of EGFL7. The EGFL7 gene encodes a 30 kDA protein with a EGF domain. miR-126 is located within intron 7 of the EGFL7 gene.

Recent studies have shown that miR-126 plays a part in vascular development and it has also been implicated in cardiovascular disease and cancer formation (Nikolic et al. 2010). EGFL7 is almost exclusively expressed by the endothelium and expression is highest in proliferating endothelial cells during embryogenesis. Most adult tissues express EGFL7 in a subset of vessels but levels are considerably lower than in the embryo. Increased levels of expression are observed during endothelial regeneration in response to injury, suggesting a role for EGFL7 in physiological and pathological angiogenesis during adult life. The egfl7 protein is secreted by the endothelial cells and deposited in the extracellular matrix (ECM) where it affects nearby endothelial cells (Nichol & Stuhlmann 2012). In summary, the temporal and spatial expression of EGFL7 suggests a role for this protein in blood vessel formation and remodeling.

1.4.1 Role of EGFL7 in vascular development

The first definite evidence that EGFL7 played an important part in vascular development came from a study on vascular tube formation in zebrafish. During vasculogenesis, cells do not directly assemble into tubes but rather make cord-like structures. Tube formation is the process wherein those cord-like structures acquire a vascular lumen due to the re-localization and modifications of cell junctions. This cord-to-tube transition was impaired in zebrafish that had a deletion of the EGFL7 gene. More specifically, angioblasts did not segregate and retained cell junctions where the vascular lumen should have formed. This led to the formation

of vessels with severely disorganized lumens or none at all. The underlying molecular mechanism on how EGFL7 affects tube formation has not been established. However, further studies indicate that EGFL7 creates a microenvironment that promotes the motility of endothelial cells during tubulogenesis. It is also possible that EGFL7 promotes the migration of endothelial cells by maintaining the correct spatial formation of the cells in the vessel (Nikolic et al. 2010).

Due to the possible role of EGFL7 in tubulogenesis it seemed likely that this factor played a similar role in angiogenic sprouting. Sprouting proceeds through the coordinated actions of two cell types: tip and stalk cells. The tip cells have filipodia that sense and migrate towards a VEGF gradient. The stalk cells proliferate to support elongation of the sprout (Nichol & Stuhlmann 2012). The tip and the stalk cells organize within a single cell layer during this sprouting process. However, In EGFL7 knock-out mice both tip and stalk cells form multiple cell layers. The ECM molecule collagen IV that is typically located in the basal membrane was found between adjacent endothelial cells in these multiple cell layers. This indicates that endothelial cells that lack EGFL7 fail to properly detect sprout boundaries. Studies have shown that EGFL7 promotes weak adhesion between cells and it is likely that the presence of EGFL7 creates an environment where endothelial cells can easily attach and detach until they are properly positioned (Parker et al. 2004). Another way in which EGFL7 could affect cell migration is through remodeling of the ECM. The egfl7 protein is deposited into the ECM and there it can inhibit the deposition of elastic fibers by repressing the conversion of tropoelastin into mature elastin. This affects the rigidity of the ECM which could in turn affect cell migration and invasion (Nichol & Stuhlmann 2012). In summary, EGLF7 controls blood vessel formation by promoting endothelial cell migration, proliferation and adhesion, as is shown by the vascular deformities that arise when levels of egfl7 are abnormal.

1.4.2 EGFL7 and the Notch signaling pathway

New studies have shed light on the molecular mechanisms that underlie EGFL7-mediated control of vascular development. Recently, a link between EGFL7 and the Notch signaling pathway has been unraveled (Schmidt et al. 2009). Signaling in the Notch pathway proceeds through ligand binding to a Notch receptor resulting in the release of the Notch intracellular domain (NICD). The NICD is then transported into the nucleus where it activates transcription of its target genes (Bray 2006).

The Notch signaling pathway plays an important role in angiogenesis by affecting tip-stalk decision during angiogenic sprouting. The tip cells in the sprout express high levels of the Notch ligand Dll4 and this ligand activates Notch receptors on the stalk cells. It is believed that the activation of this pathway causes the stalk cells to express fewer VEGF receptors and become less sensitive to the VEGF gradient. Another Notch ligand called Jagged1 is exclusively expressed in the stalk cells and this ligand competes with Dll4 to act as an antagonist for Notch receptor activation (Figure 3). Therefore, overexpression of Jagged1 leads to increased angiogenesis and tip cell numbers (Nikolic et al. 2010).

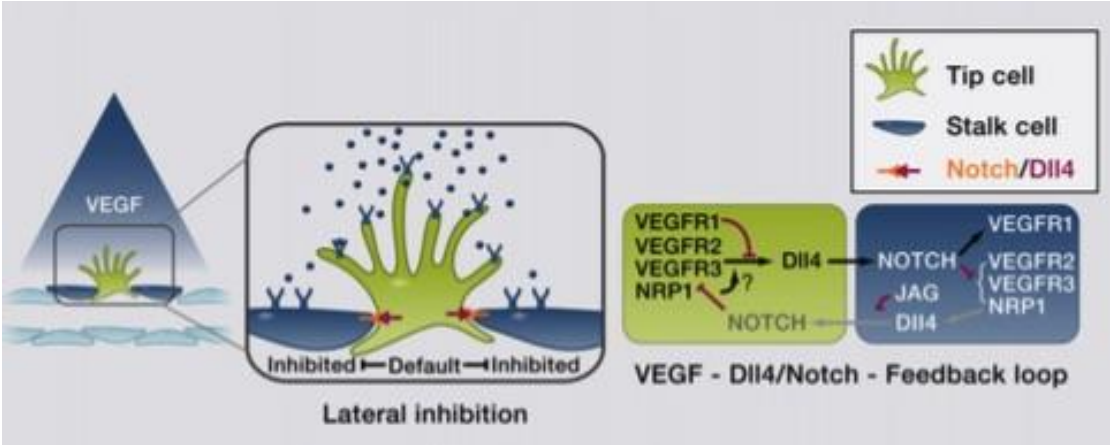

Figure 3: Notch signaling pathway in angiogenesis. The Notch signaling pathway is vital for tip-stalk decision during angiogenic sprouting (Potente et al 2013).

Research has shown that egfl7 can modulate this pathway, presumably by ECM bound egfl7 that can signal the Notch receptors on endothelial cells. Overexpression of EGFL7 reduces expression of Notch target genes, which suggests that EGFL7 is an antagonist of the Notch pathway. EGFL7 knockdown in HUVECs results in inhibition of endothelial cell proliferation, sprout formation and migration and similar results were obtained when the Notch pathway was activated in human cultured endothelial cells (Nichol & Stuhlmann 2012). Recent studies have shown that EGFL7 can compete with Jagged1 to bind the Notch receptor and hinder the Notch pathway. Taken together, these findings suggest that EGFL7 can affect vascular Notch signaling during angiogenic sprouting (Nikolic et al. 2010).

1.4.3 miR-126 in angiogenesis

Recently miR-126, which is located within intron 7 of the EGFL7 gene, has been implicated as an important factor in angiogenesis. The effect of miR-126 on vascular development has been studied by loss-of-function experiments in both zebrafish and mouse models. Loss of miR-126 in zebrafish resulted in loss of vascular integrity and hemorrhaging during embryogenesis (Fish et al. 2008). Similarly, loss of miR-126 in mice resulted in leaky vessels due to loss of vascular integrity, hemorrhaging and defects in endothelial cell migration, proliferation and angiogenesis (Wang et al. 2008). In both models, miR-126 was found to regulate the endothelial cell response to VEGF by directly repressing negative regulators of the VEGF pathway. miR-126 repressed SPRED1 and PIK3R2, which negatively regulate the VEGF pathway via the MAP kinase and PI3 kinase pathways (Nikolic et al. 2010). Previous deletion studies of the EGFL7 gene most likely affected the transcription of miR-126. Because recent studies have shown that a loss of miR-126 results in a phenotype similar to the phenotype described when loss of egfl7 was studied, concerns have been raised that the initial results were not due to loss of egfl7 but solely due to the loss of miR-126. To address this problematic issue, the separate effects of miR-126 and EGFL7 in vascular development were studied further. In the mouse model, mice that lacked the egfl7 protein but had normal levels of miR-126 had no evident vascular deformities. This could indicate that the abnormal vascular phenotypes obtained in earlier mouse studies, when EGFL7 was knocked out, were exclusively due to the loss of miR-126. However, the lack of vascular deformities could also be due to up-regulation of the EGFL7 homolog EGFL8 (Nikolic et al. 2010). EGFL7 or miR-126 knock out results in similar but distinct phenotypes in the zebrafish. If EGFL7 is lost, vessel lumens are not formed during tubulogenesis (Parker et al. 2004). However, if miR-126 is lost, lumens are formed but collapse later in embryogenesis. Therefore, it is likely that the

results obtained in the original zebrafish study were at least partly due to loss of EGFL7 (Nikolic et al. 2010). The functional relationship between EGFL7 and miR-126 is still not clear and further studies into how these two factors work together in vascular development are necessary.

1.5 The TGFβ superfamily affects vascular development: TMEM100 and Smad6

Factors of the TGFβ superfamily have been shown to regulate proliferation, migration and differentiation of endothelial cells. Furthermore, genetic studies in humans have revealed a vital role for the TGFβ family and its signaling components in angiogenesis. Members of the TGFβ superfamily exert their function by binding to specific transmembrane type I and type II serine/threonine kinase receptors. When a ligand binds the type II receptor it recruits and phosphorylates the type I receptor, also known as activin receptor-like kinase (ALK). This leads to a conformational change in the ALK receptor and in turn ALK can propagate the signal inside the cell via specific effectors. The effector molecules that play a vital role in TGFβ transduction are called Smads. When ALK is activated, it phosphorylates a Smad molecule inside the membrane and after phosphorylation the Smads are transported into the nucleus where they activate transcription of their target genes (Figure 4) (Bertolino et al. 2005).

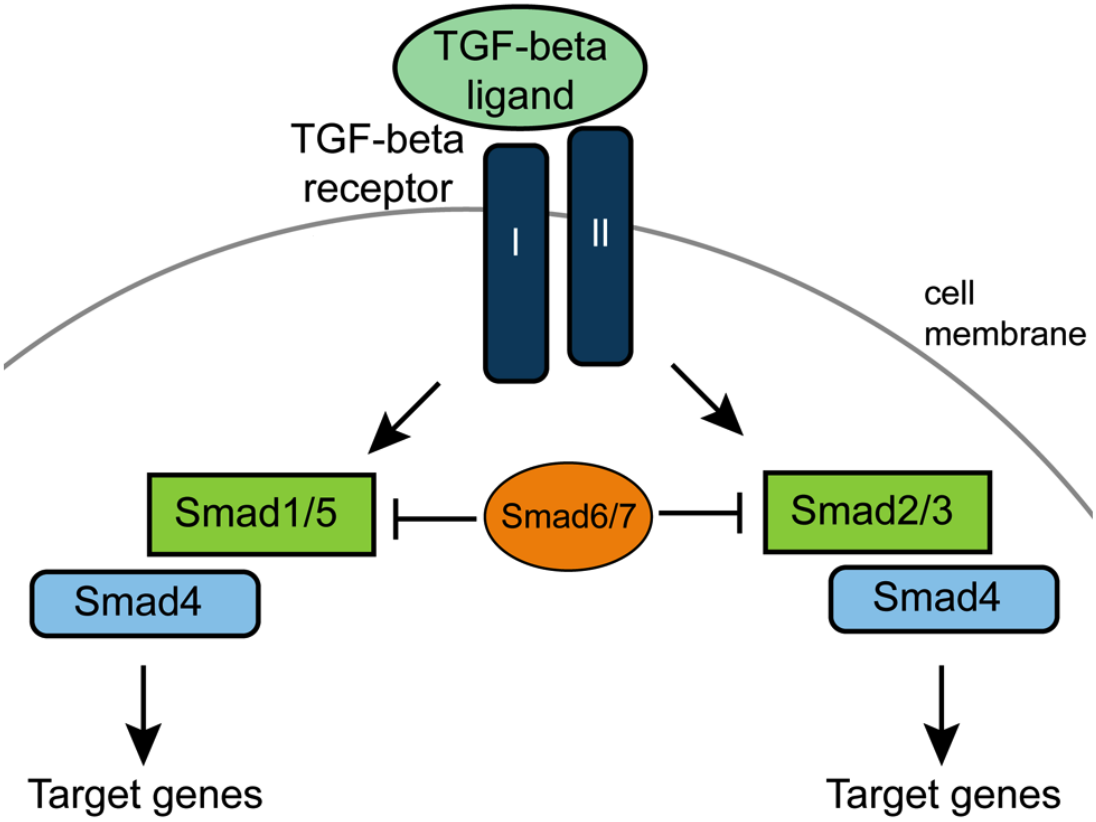

Figure 4. Schematic overview of the TGFβ signaling pathway. Type II TGFβ receptor binds its ligand and recruits the type I receptor. This leads to phosphorylation of Smad molecules and their transport into the nucleus. There they can activate the transcription of target genes. Image retrieved from: http://www.devbio.biology.gatech.edu/?page_id=7885 on the 7th of May, 2015.

During angiogenesis, Bone morphogenic factor 9 (BMP9) of the TGFβ family can bind to the ALK1 receptor and this BMP9/ALK1 signaling can result in an activating or inhibiting effect on angiogenesis. However, the molecular mechanism that controls this angiogenic effect is still unclear (Suzuki et al. 2010). Recently, the previously uncharacterized intracellular transmembrane protein TMEM100 was identified as a target downstream of BMP9/ALK1 binding. TMEM100 is expressed in arterial endothelial cells during vascular development in mouse embryos and TMEM100 null mice displayed embryonic lethality due to impaired differentiation of endothelial cells and abnormalities in vascular morphogenesis. Notch mediated signaling was found to be suppressed in TMEM100 null mice and down-regulated in ALK1 null embryos (Somekawa et al. 2012). Suppressing signaling via the Notch pathway greatly affects angiogenesis as has been detailed in a previous chapter (chapter 1.4.2). Elucidating a clearer molecular function for TMEM100 is critical to understand better how TMEM100 conveys BMP9/ALK1 signaling downstream in proper endothelial differentiation.

As previously stated the Smad molecules play a vital role in TGFβ signal transduction. When BMP9 binds the ALK1 receptor it induces phosphorylation of various Smads, which then translocate into the nucleus to active transcription. More specifically, Smad1 is phosphorylated when BMP9 binds ALK1 and then forms a complex with Smad4, which is trans-located into the nucleus (Scharpfenecker et al. 2007). BMP9 has also been shown to induce expression of the inhibitory Smad6 (Larrivée et al. 2012). Smad6 acts as an inhibitor of Smad transcription activation by competing with Smad4 to form a Smad1-Smad6 complex. This complex is inactive and does not trigger the expression of BMP responsive genes (Hata et al. 1998). The role of Smad6 in angiogenesis has not been extensively studied and more research is needed to clarify how Smad6 can affect vascular development. A possible role for Smad6 in angiogenesis could be the indirect regulation of the Notch pathway in tip cells during angiogenic sprouting through inhibition of BMP9 signaling. BMP9/ALK1 signaling activates the Notch pathway and this pathway is highly active in sprouting stalk cells but less so in tip cells as previously detailed (Larrivée et al. 2012). However, the role of Smad6 in vascular development is still largely unclear and further research into how this antagonist of BMP9 signaling could affect the vasculature is needed.

2 Project aim

This research project was part of a bigger project conducted by Guðrún Valdimarsdóttir's research group. The group is studying the connection between the TGFβ family, EGFL7 and miR-126 in endothelial differentiation of human embryonic stem cells (hESCs). The aim of this project was to study whether miR-126 could bind the 3'UTR sequence of EGFL7, TMEM100 and Smad6. Little is known about miR-126 targets in hESCs but *in silico* data indicates that EGFL7, TMEM100 and Smad6 may be targets of miR-126.

The project is divided into two main parts:

1. Generation of the 3'UTR luciferase reporter plasmids that contain the 3'UTR sequence of EGFL7, TMEM100 and Smad 6, respectively.

The first aim of this project was to create a 3'UTR reporter pISO plasmid by cloning the 3'UTR sequence of EGFL7, TMEM100 or Smad6 into the plasmid behind a luciferase erporter gene. E.*coli* cells were then transformed to make more copies of the plasmids. Finally, the plasmids were verified with the use of specific restriction enzymes and DNA sequencing.

2. HEK cells transfected with reporter plasmid and miR-126 binding assessed according to luciferase activity.

The second aim of this project was to transfect human embryonic kidney (HEK) cells with the reporter plasmid. The HEK cells were then overexpressed with miR-126 and the binding capacity of miR-126 to the 3'UTR sequences was assessed according to luciferase activity (Figure 5).

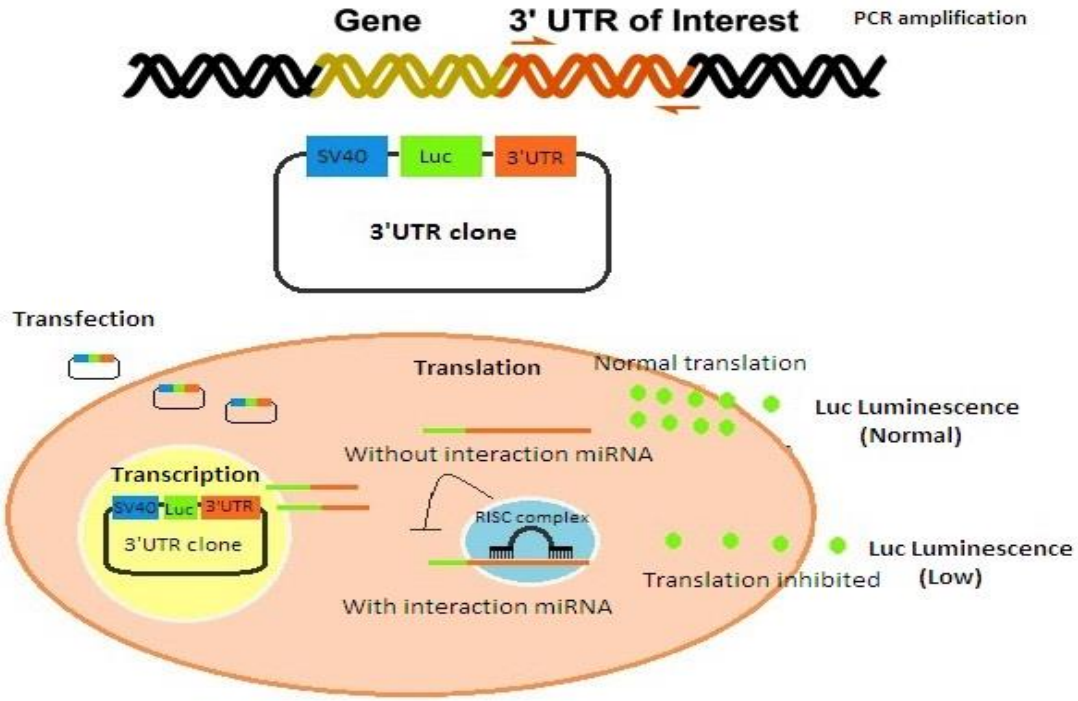

Figure 5. Overview of 3'UTR luciferase reporter plasmid function. Image retrieved from: http://www.genecopoeia.com/product/mirna-targets/ on the 9th of May, 2015.

3 Materials and Methods

3.1 Generation of luciferase reporter plasmids

3.1.1 PCR amplification of the 3'UTR sequences of EGFL7, TMEM100 and Smad6

The first step of the reporter plasmid generation was to amplify the 3'UTR sequences of EGFL7, TMEM100 and Smad6. A polymerase chain reaction (PCR) was performed to amplify the 3'UTR sequences of EGFL7, TMEM100 and Smad6 from human genomic DNA. The specific primers were designed using the Primer Blast database Primer 3 (primer3.ut.ee). In addition, the restriction sites for the restriction enzymes SacI and NheI were added, along with the motif GGTGGT to protect the sequences from 5' exonuclease activity. The primers were manufactured by Biomers, Germany and the sequences are shown in table 1.

Table 1. Sequence of primers for the 3'UTR sequences of EGFL7, TMEM100 and Smad6. The restriction sites for the enzymes SacI and NheI are underlined.

Name	Sequence (5'-3')	PCR product size [bp]
hEGFL7 + Luc fw	GGTGGTGAGCTCGACCTTCGCCTCATCCAAC	443
hEGFL7 + Luc rev	GGTGGTGCTAGCTGACACAGCAGCTCACGTTT	
hTMEM100 + Luc fw	GGTGGGTGAGCTCAAGAAAGCCAAGAGACGGGA	1198
hTMEM100 + Luc rev	GGTGGTGCTAGCTGCTGGCATACGTGTTAAGC	
hSmad6 + Luc fw	GGTGGTGAGCTCCCTCCTCAACAACCCCAGAT	622
hSmad6 + Luc rev	GGTGGTGCTAGCTCCTCCCTTTTCAATTTGTTCTG	

The reaction was performed in 0.2 ml PCR tubes on ice. The PCR reaction components are shown in table 2.

Table 2. PCR reaction components. H_2O was added for a total reaction volume of 50 µl.

	Volume [µl]		
	EGFL7	**TMEM100**	**Smad6**
Genomic DNA (~500 ng/µl)	2	0.3	2
Primer fw (10 pmol/µl)	4	2.5	4
Primer rev (10 pmol/µl)	4	2.5	4
dNTPs (10 mM)	2	2	2
Polymerase	0.2[1]	0.5[1]	0.2[2]
10x buffer	5[1]	5[1]	5[2]

[1]Pfu polymerase (2.5 U/µl) and 10x Pfu buffer [2]DreamTaq polymerase (5 U/µl) and 10xDreamTaq buffer

Two PCR programs were used to amplify the 3'UTR sequences. The first program ensured that the primers could bind to the 3'UTR binding region. The second program amplified the sequence of interest.

Table 3. Programs for PCR reaction. A) First program for PCR reaction B) Second program for PCR reaction. Δ stands for temperature increase per cycle. *The starting temperature for TMEM100 was 52°C.

A

Step	Temperature [°C]	Time
1	95	5 min
2	95	45 s
3	55* + Δ0.5°C	45 s
4	72	45 s
	Cycle back to step 1 for 22 cycles	
5	72	10 min
6	4	∞

B

Step	Temperature [°C]	Time
1	95	5 min
2	95	45 s
3	60	45 s
4	72	90 s
	Cycle back to step 1 for 22 cycles	
5	72	10 min
6	4	∞

3.1.2 Agarose gel electrophoresis

After PCR amplification, the PCR products were separated according to size using gel electrophoresis. A 0.8% agarose gel was created by dissolving 0.4 g of agarose in 50 ml of 1xTAE buffer. The mixture was heated in a microwave until the agarose was completely dissolved. After the mixture had cooled down to approximately 60°C, ethidium bromide (0.6 µg/ml) was added. The mixture was then poured into a gel tray and allowed to polymerize. Afterwards, the PCR products were mixed with 6x loading dye (NEB) and loaded into gel chambers with a 100 bp ladder (NEB) as a standard of comparison. The gel was run at 60 V for 40 minutes. After electrophoresis, the bands were visualized and compared with the molecular weight standard. Fragments of the correct size were cut out of the gel and isolated using the Nucleo Spin® Gel and PCR Clean-Up kit from Macherey-Nagel. Instructions provided by the manufacturer were followed. The DNA was eluted in 30 µl of elution buffer. The DNA was then measured with NanoDrop in order to determine the DNA concentration and quality.

3.1.3 Restriction digest of pISO plasmid and 3'UTR fragments

A restriction digest was performed on the pISO plasmid and the 3'UTR fragments. The restriction enzymes NheI (NEB) and SacI (NEB) were used to cut the pISO plasmid and the ends of the 3'UTR fragments (plasmid graphic maps are shown in Appendix A). This generated sticky ends on both the pISO plasmid and the 3'UTR's. Optimal restriction conditions for the pISO plasmid are indicated in table 4 and optimal restriction conditions for the 3'UTRs are indicated in table 5.

Table 4. Restriction digestion of pISO plasmid. H_2O was added for a total reaction volume of 60 µl.

	Volume [µl]
pISO plasmid (542 ng/µl)	3.7
NheI (20000 U/ml)	2
SacI (20000 U/ml)	2
10xNEB4 buffer	6
H_2O	46.3
Total	60

Table 5. Restriction digestion of the 3'UTR fragments.

	EGFL7 (150 ng/µl)	**TMEM100 (20 ng/µl)**	**Smad6 (106 ng/µl)**
	Volume [µl]	**Volume [µl]**	**Volume [µl]**
DNA	15	15	4.7
NheI	1	1	0.2
SacI	1	1	0.2
10xCutsmart buffer	4	4	2
H_2O	19	19	11.9
Total	40	40	20

All the samples were incubated at 37°C for 30 minutes and then heat inactivated at 65°C for 20 minutes. Afterwards, the samples were run on a 0.8% agarose gel and isolated from the gel using the Nucleo Spin® Gel and PCR Clean-Up kit from Macherey-Nagel according to instructions provided by the manufacturer.

3.1.4 Ligation

To generate the reporter plasmid, the 3'UTR fragments and the linear pISO plasmid were ligated in a molar ratio of 1:3, respectively, using a ligation calculator (insilico.uni-duesseldorf). The ligation reaction components are shown in table 6.

Table 6. Ligation of pISO plasmid and 3'UTR inserts. H_2O was added for a total reaction volume of 20 µl

	EGFL7 (112 ng/µl)	**Smad6 (20 ng/µl)**		**TMEM100 (20 ng/µl)**
	Volume [µl]	**Volume [µl]**		**Volume [µl]**
pISO (40 ng/µl)	5	5	pISO (29.2 ng/µl)	3.42
Insert	0.45	3.5	Insert	3.5
T4 DNA ligase	1	1	T4 DNA ligase	1
10x T4 ligase buffer	2	2	10x T4 ligase buffer	2

The samples were ligated at 16°C overnight and then heat inactivated at 65°C for 20 minutes. The samples were stored at -20°C.

3.1.5 Heat shock transformation

The competent E.*coli* strain Top10 was transformed with the reporter plasmids that included the particular 3'UTRs to multiply the plasmids with a high copy number and to minimize mutation events using heat shock transformation. First, E.*coli* bacteria were thawed on ice. Then, 1 µg of plasmid was carefully added to 100 µl of bacteria and incubated on ice for 25 minutes. The bacteria were then heat shocked at 42°C for 45 seconds and then placed on ice for two minutes. The bacteria were incubated at 37°C in a shaker for one hour and then centrifuged at 3000 rpm for 5 minutes. After centrifugation, 800 µl of medium was removed and the bacteria were re-suspended in the left over medium. Subsequently, the bacteria were plated on LB agar plates (2g BactoTryptone (BD Biosciences), 1g BactoYeast (BD Biosciences), 2g NaCl (Sigma), 3g BactoAgar (BD Biosciences) in 200 mL H_2O) containing 50 µg/ml ampicillin and incubated at 37°C overnight. After incubation, eight bacterial colonies from each plate were picked and further incubated in 2.5 ml LB medium (2g BactoTryptone (BD Biosciences), 1g BactoYeast (BD Biosciences), 2g NaCl (Sigma) in 200 mL H_2O) containing 50 µg/ml ampicillin at 37°C overnight. This was done to maximize the amount of plasmid available. Afterwards, the plasmids were isolated from the bacteria using a DNA, RNA and protein purification Nucleospin® plasmid kit from Macherey-Nagel according to manufacturers instructions.

3.1.6 Verification of the pISO reporter plasmid

Restriction digests were performed to identify which plasmids contained the 3'UTR insert. To identify the EGFL7 reporter plasmids the restriction enzyme SacI (NEB) was used. Two different restriction digests were necessary to identify the TMEM100 reporter plasmids, namely the SacI (NEB) and NheI (NEB) were used for the first digest and the restriction enzyme HindIII (NEB) for the second digest. To identify the Smad6 reporter plasmids the restriction enzymes XhoI (NEB) and NheI (NEB) were used (done by Dr. Anne Richter). A pISO plasmid without an insert and an undigested pISO plasmid were both used as controls. Optimal restriction conditions for each digestion are indicated in table 7.

Table 7. Restriction digestion of reporter plasmids. H_2O was added for a total reaction volume of 20 µl

	EGFL7	**1st digestion TMEM100**	**2nd digestion TMEM100**	**Smad6**
	Volume [µl]	**Volume [µl]**	**Volume [µl]**	**Volume [µl]**
DNA (~500 ng)	3	2	2	1.5
SacI (20000 U/ml)	0.3	0.3	-	0.3
NheI (20000 U/ml)	-	0.3	-	0.3
HindIII (20000 U/ml)	-	-	0.3	-
10x Cutsmart buffer	2	2	2	2

The samples were incubated at 37°C for one hour and then heat inactivated at 65°C for 20 minutes.

After the restriction digest the samples were analyzed with agarose gel electrophoresis (see section 3.2.1). All the samples were run on a 0.8% agarose gel.

3.1.7 DNA sequencing

Plasmids that showed the right digestion pattern were sequenced in order to determine the exact sequence of the analyzed reporter plasmids that contained the 3'UTR inserts. The samples were prepared according to Beckman Coulter Genomic instructions and sent out for sequencing to Beckman Coulter Genomics, Great Britain (https://myproject.beckmangenomics.com/myp/uwa.maya.engine.MayaEngine?siteid=col&mapid=home). The sequences were analyzed using the BioEdit Sequence Alignment Editor software version 7.1.9 (done by Dr. Anne Richter).

3.2 Cell culture and maintenance of HEK cells

HEK293T cells were used in this study (obtained from The Netherlands Cancer Institute, Amsterdam, Holland). The cells were cultured in MEF medium (table 8).

Table 8. MEF medium composition.

MEF medium	Concentration
DMEM (11960-044) (Invitrogen)	
Fetal Bovine Serum (Sigma)	10%
Penicillin/Streptomycin (Invitrogen)	50 U/ml
Streptomycin (Invitrogen	50 µg/ml
GlutaMAX (Invitrogen)	2mM

The cells were passaged when they reached a confluence of 70-90%. The MEF growth medium, PBS and TrypLE had to be pre-warmed in an incubator at 37°C before the cells could be passaged. The cells were then washed once with 3 mL of 1xPBS (Invitrogen) and treated using 1 mL of TrypLE. Afterwards, the cells were incubated at 37°C for 5 minutes. After incubation, the TrypLE was inactivated by adding 4 mL of MEF growth medium, and the cell suspension was centrifuged at 465 rpm for 5 minutes to pellet the cells. Finally, the supernatant was removed and the cells were re-suspended in MEF growth medium and split in a ratio of 1:8. - 1:15. The cells were counted using a Neubauer chamber.

3.3 Transfection of HEK293T cells

The HEK293T cells were seeded onto a 96 well culture plate. In total, 24 wells were prepared by adding $1{,}0x10^4$ cells per well using 100 µl of MEF medium and the cells were incubated at 37°C overnight. The cells were transfected using Fugene HD (Promega) according to manufacturer's instructions. After testing of several DNA concentrations and different ratios between DNA and transfection reagent (Fugene), 100 ng of the reporter plasmid and a 1:3 ratio (DNA to Fugene reagent) were used per 96-well. Each construct was added in a triplicate. The prRL plasmid (bearing a GFP construct) was used as a transfection control to verify transfection efficiency. The cells were incubated at 37°C for three hours. Afterwards, the medium was changed to MEF culture medium and the cells were incubated at 37°C overnight. Untransfected cells were used as a control.

3.4 mIR-126 infection and starvation

The HEK293T cells were infected with a miR-126 overexpression lentiviral construct. The medium was then removed and 40 µl of MEF growth medium and 40 µl of miR-126 lentiviral solution, respectively, were added to each well. Polybrene (Invitrogen) was added to a final concentration of 10 µg/ml per well. The cells were incubated at 37°C and the medium was changed 24 hours later using MEF medium.

3.5 Luciferase assay

The Dual-Glo® Luciferase Assay System from Promega was used to quantitate the luminescent signal from each report construct. Instructions provided by the manufacturer were followed. To measure the luciferase activity, 50 µl of LARII reagent was added to each well and incubated for ten minutes. To measure the Renilla luciferase activity, 50 µl of Stop & Glo® reagent was added to each well and incubated for ten minutes. The light produced was measured using a Domulus™II Microplate Multimode Reader.

3.6 Calculation of luciferase assay results

The Dual-Glo® Luciferase Assay System makes it possible to accurately calculate the luciferase activity by correcting for the effects of differences in transfection efficiency. The Renilla reagent is used to detect the transfection efficiency and by subtracting the Renilla activity from the luciferase activity it is possible to accurately calculate the luciferase activity in each sample. After calculating the luciferase activity, the mean and standard deviation of the three samples for each construct was calculated. A student's T-test was used to determine whether the results were statistically significant.

4 Results

During endothelial development the expression of many different genes must be precisely regulated to ensure the correct formation of the capillary network. Research has shown that the genes EGFL7, TMEM100 and Smad6 as well as the microRNA miR-126 play a role in endothelial development. Furthermore, *in silico* data indicates that EGFL7, TMEM100 and Smad6 may be targets of miR-126. The focus of this study was to determine whether miR-126 could bind to the 3'UTR sequences of these three genes. For this purpose, reporter plasmids that contained the 3'UTR sequence of EGFL7, TMEM100 or Smad6 behind a luciferase reporter gene were created. HEK293T cells that overexpressed miR-126 were then transfected with the reporter plasmid and the binding of miR-126 was assessed according to luciferase activity in the transfected cells. An overview of the experimental work flow is shown in figure 6.

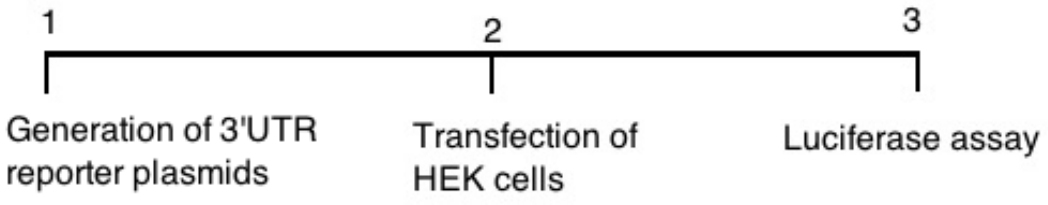

Figure 6. Overview of the experimental workflow.

4.1 Generation of reporter plasmids

The first aim of this study was to create a reporter plasmid that contained the 3'UTR sequence of EGFL7, TMEM100 and Smad6, respectively. The first step of creating the plasmids was to amplify the 3'UTR sequences of EGFL7, TMEM100 and Smad6 from human genomic DNA. To verify that the correct sequences had been amplified the sequences were analyzed with electrophoresis, and the band size was compared to the expected size of the sequence. The expected size of the 3'UTR EGFL7 sequence was 443 bp. The 3'UTR EGFL7 band was located in between the 500 bp and 400 bp band of the 100 bp ladder, used for comparison. This indicated that the amplified sequence had the correct size and the correct sequence had been amplified (Figure 7). The 100 bp ladder transferred into the next well and therefore faint bands can be seen in that well. The lower and less distinct band is due to primer dimers.

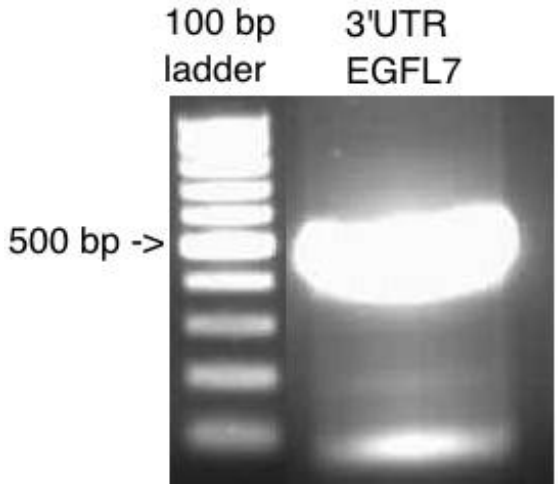

Figure 7. Gel electrophoresis analysis of 3'UTR EGFL7. The expected size of the 3'UTR EGFL7 band was 443 bp. The band is located in between the 500 bp and 400 bp bands on the 100 bp ladder used for comparison, indicating that the correct sequence had been amplified. The lower band is due to primer dimers.

Electrophoresis analysis also confirmed that the 3'UTR TMEM100 and 3'UTR Smad6 sequences had the correct size and the correct sequences had been amplified (data now shown).

The pISO plasmid was digested using the same restriction enzymes as the 3'UTR fragments to generate sticky ends so that the 3'UTR fragments could be cloned into the pISO plasmid. Electrophoresis analysis was performed to verify the size of the digested pISO plasmid. The expected size of the digested pISO plasmid is 5228 bp. The digested pISO band is located close to the 5000 bp band of the 1 kb ladder used as comparison, indicating the correct size of the pISO plasmid (Figure 8). A sample of undigested pISO plasmid was used as comparison and the different sizes of the bands are due to differences in coiling of the plasmid structure.

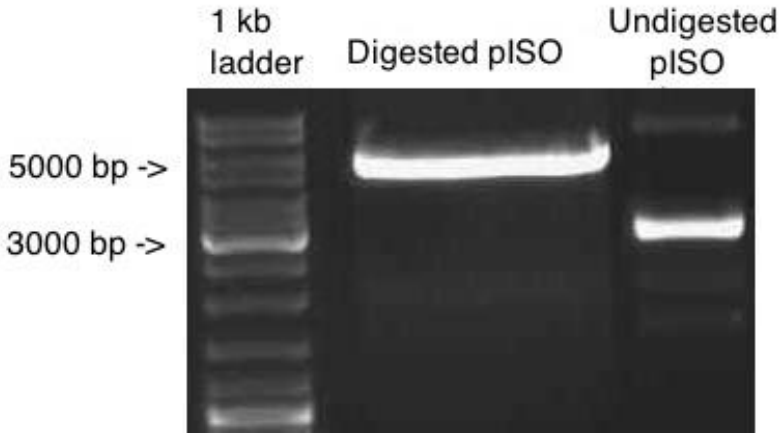

Figure 8. Gel electrophoresis analysis of pISO plasmid. The expected size of the digested pISO fragment is 5228 bp. The band is located close to the 5000 bp band on the 1 kb ladder used for comparison indicating a correct size. An undigested pISO plasmid was used as comparison.

The electrophoresis analysis confirmed that the correct 3'UTR sequences of EGFL7, TMEM100 and Smad6 had been amplified. The 3'UTR fragments and the pISO plasmid were then cut out of the gel, purified and the DNA concentration was measured. These fragments were then ligated together to generate the luciferase reporter plasmids with 3'UTR inserts.

4.1.1 Verification of pISO + 3'UTR reporter plasmids

The pISO plasmid and the 3'UTR sequences of EGFL7, TMEM100 and Smad6, respectively, were ligated together to make a reporter plasmid that contained a 3'UTR insert in front of a luciferase reporter gene. To determine whether the plasmids had incorporated the 3'UTR insert of interest, restriction digests were performed at different restriction sites including sites within the insert itself (Appendix A). The digested samples were then analyzed with electrophoresis to identify the samples that showed the correct digestion pattern. The reporter plasmids that had incorporated the 3'UTR EGFL7 insert should display two bands after the restriction digest using the restriction enzyme SacI. The larger band should be 5362 bp and the smaller band should be 332 bp. The sample in well 2 showed the correct digestion pattern (Figure 9). The larger band is located above the 4361 bp band of the λDNA/HindIII ladder and the second band is located below the 500 bp band of the 100 bp ladder. The clone that had incorporated the insert is marked with a * and the insert is indicated within the red box.

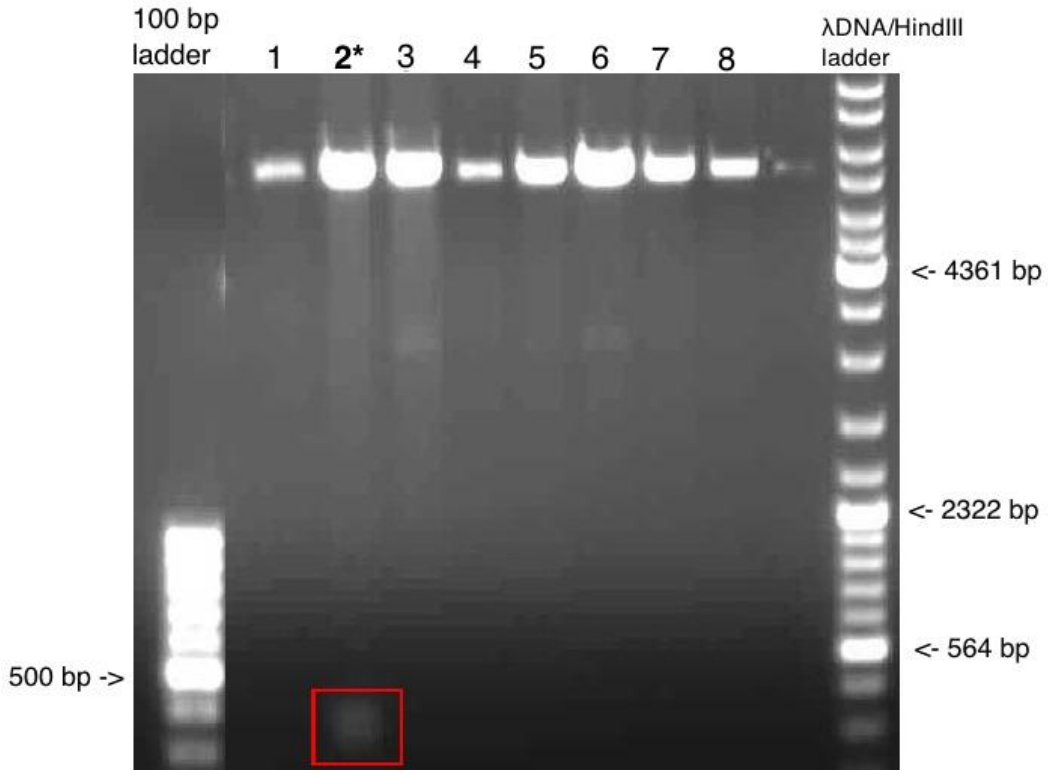

Figure 9. Gel electrophoresis analysis of pISO + 3'UTR EGFL7 plasmids. Restriction digest of the reported plasmid should produce two bands with the size 5362 bp and 332 bp. Plasmids that had incorporated the insert are marked with * and the insert is indicated within the red box.

The plasmids that had incorporated the 3'UTR TMEM100 insert should display two bands after the restriction digest using the restriction enzymes SacI and NheI. The larger band should be 5237 bp and the smaller band should be 1148 bp. Four clones showed the correct

digestion pattern, the larger band was located a just below the 6557 bp band of the λDNA/HindIII ladder and the smaller band was located close to the 1000 bp band of the 100 bp ladder (Figure 10). The clones that had incorporated the insert are marked with a * and the inserts are indicated within the red boxes.

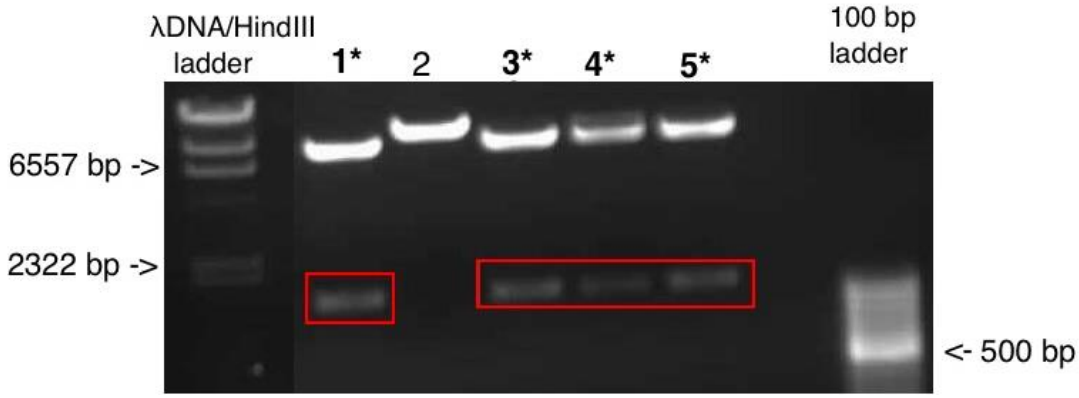

Figure 10. Gel electrophoresis analysis of pISO + 3'UTR TMEM100 plasmids. Restriction digest of the reporter plasmid should display two bands with the size 5237 bp and 1148 bp. Plasmids that had incorporated the insert are marked with * and the inserts are indicated within the red boxes.

The plasmids that had incorporated the 3'UTR Smad6 insert should display two bands after the restriction digest using the restriction enzymes NheI and XhoI (done by Dr. Anne Richter). The bigger band should be 5321 bp and the smaller band should be 542 bp. Three clones showed the right digestion pattern, the larger band was located close to the 5000 bp band of the 1 kb ladder and the smaller band was located close to the 500 bp band of the 100 bp ladder (Figure 11). The clones that had incorporated the insert are marked with a * and the inserts are indicated within the red boxes.

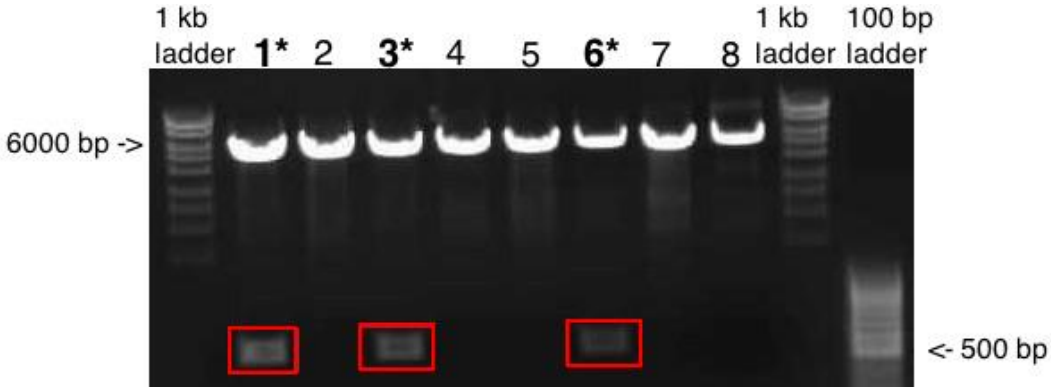

Figure 11. Gel electrophoresis analysis of pISO + 3'UTR Smad6 plasmids. Restriction digest of the reporter plasmid should display two bands with the size 5321 bp and 542 bp. Plasmids that had incorporated the insert are marked with * and the inserts are indicated within the red boxes.

The plasmids that showed the correct digestion pattern were sent out for sequencing.

4.1.2 Sequencing

To determine the exact DNA sequences of the plasmids that showed the right digestion pattern, the plasmids were sent out for sequencing (done by Dr. Anne Richter). Analysis of the sequences showed that the TMEM100 and Smad6 3'UTR inserts contained the putative binding site for miR-126 (sequences are shown in appendix B). However, all of the plasmids that had incorporated the EGFL7 3'UTR insert had either incorporated

inverted or repeated inserts with mutations in the putative binding site for miR-126. One clone had incorporated a part of the 3'UTR EGFL7 sequence twice and contained two miR-126 putative binding sites (Figure 12). The small letters of the sequence are the pISO plasmid backbone and the capital letters are the EGFL7 3'UTR fragment. The sequences highlighted in yellow depict the start of the EGFL7 3'UTR fragment and the sequences highlighted in green depict the putative binding site for miR-126.

Figure 12. 3'UTR EGFL7 insert with two miR-126 putative binding sites. The small letters of the sequence are the pISO plasmid backbone and the capital letters are the 3'UTR fragment. The sequences highlighted in yellow are the start of the 3'UTR sequence of EGFL7 and the sequences highlighted in green are the putative binding site for miR-126.

The reporter plasmids that had incorporated the TMEM100 and Smad6 3'UTR inserts with the putative binding site for miR-126, could be used for the transfection of the HEK cells and the luciferase assay. Because it proved difficult to create an EGFL7 reporter plasmid that contained one putative binding site for miR-126, the clone that contained the two binding sites was used in further experiments.

4.2 Transfection efficiency in HEK293T cells

Before the HEK293T cells could be transfected with the reporter plasmids it was necessary to determine which ratio between DNA and the transfection reagent (Fugene) provided both good transfection efficiency and low cytotoxicity to the cells. For this purpose, the HEK293T cells were transfected with a prRL plasmid in three different ratios of DNA and Fugene (1:2, 1:3 and 1:4). The cells were examined 24 hours and 48 hours after transfection. Cytotoxicity was determined by assessing cell morphology and the amount of dead cells in the medium. The transfection efficiency was ascertained both by amount of transfected/fluorescent cells and fluorescence intensity. The number of dead cells and the transfection efficiency were valued by a score system: lowest (+) to highest (+++) cell number or efficiency (Table 9).

Table 9. Transfection efficiency and cytotoxicity.

Ratio (DNA:Fugene)	Transfection efficiency	Dead cells
1:2	+	+
1:3	++	++
1:4	+++	++++

The cells transfected with a low amount of Fugene (1:2 ratio) had good cell quality with a low number of dead cells in the medium (score: +) but the transfection efficiency was very low (score: +). A higher ratio of Fugene to DNA (1:3) resulted in higher transfection efficiency (score: ++) with a moderate amount of dead cells in the medium (score: ++) (Figure 13). The highest ratio of Fugene to DNA (1:4) resulted in very high transfection efficiency (score: +++) but poor cell quality with stressed and enlarged cells containing many vacuoles and a high number of dead cells (score: +++).

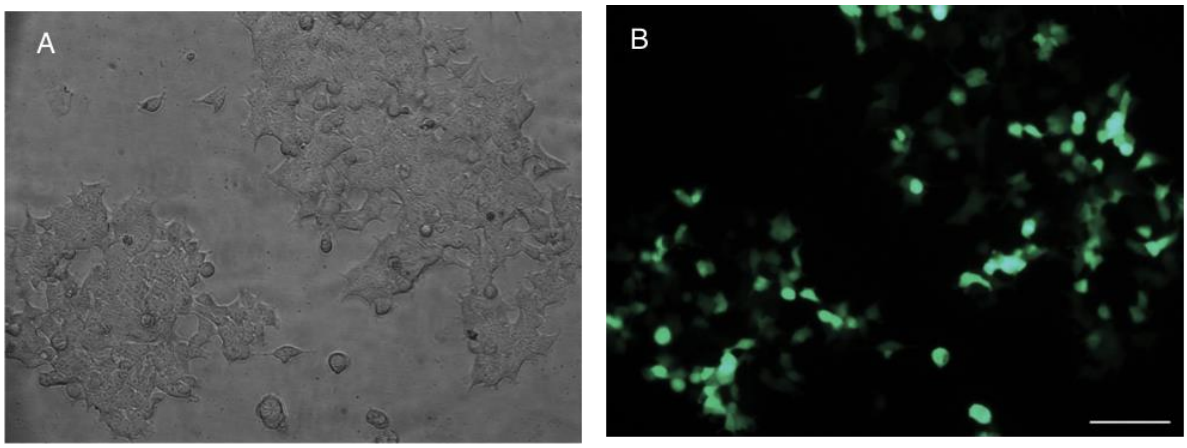

Figure 13. Detection of transfection efficiency. (A) Brightfield and (B) Immunofluorescent staining. Cells were transfected with a ratio of 1:3 (DNA:Fugene) and examined for dead cells, amount of transfected cells and fluorescence intensity 48 hours after transfection. Bar represents 100 μm and exposure time is 78.4 ms.

The ratio of 1:3 of Fugene to DNA provided both a good transfection efficiency and low cytotoxicity to the cells with a moderate amount of dead cells and was therefore applied in the following experiments (Figure 13).

4.3 Luciferase assay

To determine whether miR-126 could bind to the 3'UTR sequences of EGFL7, TMEM100 and Smad6, HEK293T cells were transfected with the previously generated 3'UTR luciferase reporter plasmids that contained the putative binding site for miR-126. The cells were lentivirally infected with either a miR-126/pLVTHM expression vector or a pLVTHM control vector 24 hours after transfection. Then, binding was assessed by measuring the luciferase activity in the transfected cells. If miR-126 binds to the 3'UTR sequences of EGFL7, TMEM100 or Smad6, the luciferase activity should be reduced, because of a faster RNA-degradation and translational inhibition.

The luciferase assay was performed using the Dual-Glo® Luciferase Assay system which both measures luciferase activity and corrects for the effect of different transfection efficiencies in the cells using renilla activity. The pISO plasmid without a 3'UTR insert was used as a control. The luciferase assay showed that the HEK293T cells transfected with reporter plasmids containing the 3'UTR inserts of EGFL7 and Smad6, respectively, resulted in reduced luciferase activity compared to the pISO plasmid without insert. The HEK293T cells that were transfected with the TMEM100 3'UTR reporter plasmid did not show reduced luciferase activity compared to the pISO control (Figure 14)

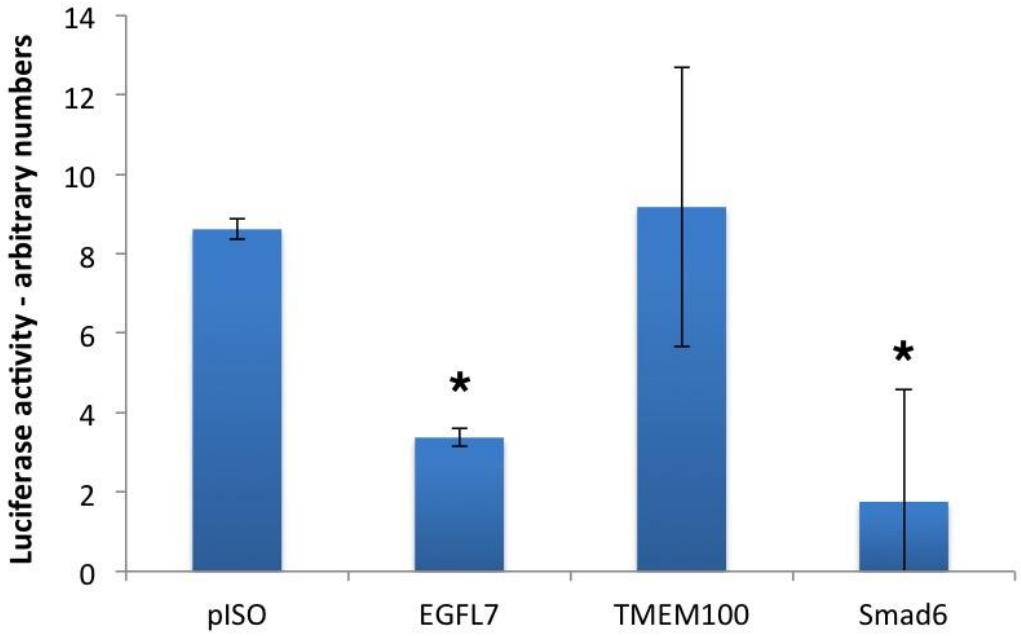

Figure 14. Luciferase assay reflecting miR-126 binding affinity to 3´UTRs. The pISO plasmid without an insert was used as a control. The luciferase assay showed decreased luciferase activity in the HEK cells transfected with plasmids containing the 3'UTR sequences of EGFL7 and Smad6, respectively. Bars represent standard deviation, * $p < 0.05$.

The p-value was calculated using an unpaired Student's *t*-test, which confirmed that the results obtained for EGFL7 and Smad6 were statistically significant. Because the reporter plasmid with the 3'UTR EGFL7 insert contained two binding sites for miR-126 these results must be taken with precaution and the experiment should be repeated with a insert containing only one binding site. Nonetheless, the results strongly indicate the miR-126 does bind to the 3'UTR sequence of EGFL7 and Smad6 but does not bind to the 3'UTR sequence of TMEM100.

5 Discussion

Endothelial development is an important process for generating new blood vessels during embryonic development, wound repair and cancer progression. Development of the endothelium is highly regulated and numerous factors and pathways that play a role in this process have been identified. Preliminary studies of the research group have indicated a connection between the BMP-Smad1/5 signaling pathway, EGFL7 and miR-126 in endothelial development but further research into how exactly these factors work together to regulate this process is needed. *In silico* data indicated that EGFL7 as well as two downstream targets of the BMP-Smad1/5 signaling pathway, TMEM100 and Smad6, could be targets of miR-126. The aim of this study was to determine whether miR-126 could bind the 3'UTR sequences of EGFL7, TMEM100 and Smad6 and therefore regulate the expression of those genes. This could provide an example of how the BMP-Smad1/5 signaling pathway, EGFL7 and miR-126 function together to regulate endothelial development. In this study I provide evidence that miR-126 binds to the 3'UTR sequences of EGFL7 and Smad6 but not TMEM100.

5.1 miR-126 binds the 3'UTR sequences of EGFL7 and Smad6

The first step of this project was to generate the 3'UTR luciferase reporter plasmids that would be used to determine whether miR-126 could bind the 3'UTR sequences of EGFL7, TMEM100 and Smad6. Reporter plasmids that contained the 3'UTR sequences of TMEM100 and Smad6 could easily be generated but it proved to be difficult to generate reporter plasmids that contained the 3'UTR sequence of EGFL7. DNA sequencing results showed that the plasmids that had incorporated the 3'UTR EGFL7 insert contained mutations, deletions or duplications in the putative binding site for miR-126, rendering them unsuitable for this study. After modifying the cloning process several times, a clone containing a 3'UTR EGFL7 insert with two putative binding sites for miR-126 was obtained. Because it had proven difficult to generate a 3'UTR EGFL7 clone with a putative binding site for miR-126 the clone with the two binding sites was used in further experiments. HEK cells were then transfected with the 3'UTR insert luciferase reporter plasmids and a luciferase assay was used to determine whether miR-126 could bind the 3'UTR sequences. The results from the assay showed that miR-126 could bind the 3'UTR sequences of EGFL7 and Smad6 but not TMEM100. Because the reporter plasmid with the 3'UTR EGFL7 insert contained two binding sites for miR-126 these results must be taken with precaution but they do nonetheless strongly indicate that miR-126 can bind to the 3'UTR sequence of EGFL7. Furthermore, in this study HEK cells were transfected with the reporter plasmids and overexpressed with miR-126 but it would be interesting to repeat the experiment using ESCs.

Previous studies have illustrated the importance of miR-126, EGFL7, TMEM100 and Smad6 in vasculo- and angiogenesis (Fish et al. 2008; Nichol & Stuhlmann 2012; Nikolic et al. 2010; Somekawa et al. 2012; Larrivée et al. 2012). It remains unclear however, whether these factors could work together in one pathway to regulate endothelial development. TMEM100 and Smad6 are downstream targets of the BMP-Smad1/5

signaling pathway and studies have shown that TMEM100 and Smad6 expression up-regulated in response to BMP9/ALK1 binding (Scharpfenecker et al. 2007; Larrivée et al. 2012). Furthermore, recent research has illustrated that EGFL7 expression is up- regulated upon BMP9-Smad1/5 activation, indicating that EGFL7 is also a downstream target of BMP9/ALK1 signaling (Masato Morikawa, personal communication). These reports suggest that EGFL7, Smad6 and TMEM100 are all downstream targets of the same signaling pathway.

In this study, EGFL7 and Smad6 were identified as targets of miR-126. microRNAs regulate gene expression post-transcriptionally by binding the 3'UTR sequence of their target mRNAs and the effects of miRNA mediated regulation of gene expression can vary tremendously, from fine-tuning to greatly altering expression levels of their target genes. Generally, miRNAs repress gene expression by destabilizing mRNAs in the cytoplasm or hindering translation of mRNAs into proteins (Fabian et al. 2010). However, recent studies have revealed that miRNAs also have the ability to activate gene expression post-transcriptionally. miRNA mediated up-regulation of gene expression is selective and regulated by the RNA sequence context, specific co-factors and cellular conditions. In addition, a single miRNA can both up- and down-regulate expression of a target gene depending on different cellular conditions and co-factors (Vasudevan 2012). Therefore, even though EGFL7 and Smad6 have been identified as targets of miR-126 and miRNAs generally down-regulate expression of their target genes, it is impossible to say whether miR-126 represses or activates expression of EGFL7 and Smad6 without further research. It is also possible that miR-126 can both function in down and up-regulation of EGFL7 and Smad6 depending on different cellular conditions during endothelial development.

As was previously mentioned, EGFL7 and Smad6 are both downstream targets of BMP9/ALK1 binding (Masato Morikawa, personal communication; Larrivée et al. 2012). Because miR-126 is located within intron 7 of the EGFL7 gene and is transcribed from the same promoters as EGFL7, levels of miR-126 likely correlate with expression levels of EGFL7 (Zhang et al. 2013). Therefore, it is unlikely that miR-126 greatly alters EGFL7 expression but the function of miR-126 could be to fine-tune levels of EGFL7 during endothelial development. Indeed, recent results gained in the research group indicate that overexpression of miR-126 leads to down-regulation of EGFL7 in hESC derived vascular cells. Smad6 is an antagonist of BMP9 signaling and BMP9 mediated up-regulation of Smad6 results in a negative feedback loop (Scharpfenecker et al. 2007). This negative feedback loop inhibits the activation of BMP responsive genes, including EGFL7. Smad6 is also a target of miR-126 and therefore miR-126 could inhibit this negative feedback loop by down-regulating Smad6 and preventing Smad6-Smad4 complex formation. In this manner, miR-126 could both affect expression of Smad6 directly and EGFL7 expression indirectly by repressing the negative feedback loop. Moreover, miRNAs have been shown to function in a time and dose dependent manner (Shu et al. 2012). Therefore, miR-126 could down-regulate expression of Smad6 at a specific dose and time and thus up-regulate EGFL7 indirectly by hindering the inhibition of BMP9/ALK1 signaling. Higher expression levels of EGFL7 would in turn lead to higher levels of miR-126 which could then start to target EGFL7 to fine tune its expression. Additionally, repression of Smad6 could allow miR-126 to affect its own transcription via EGFL7 expression.

Taken together, these results provide an example of how EGFL7, TMEM100, Smad6 and miR-126 could function together in one common regulatory pathway, during endothelial development (Figure 15).

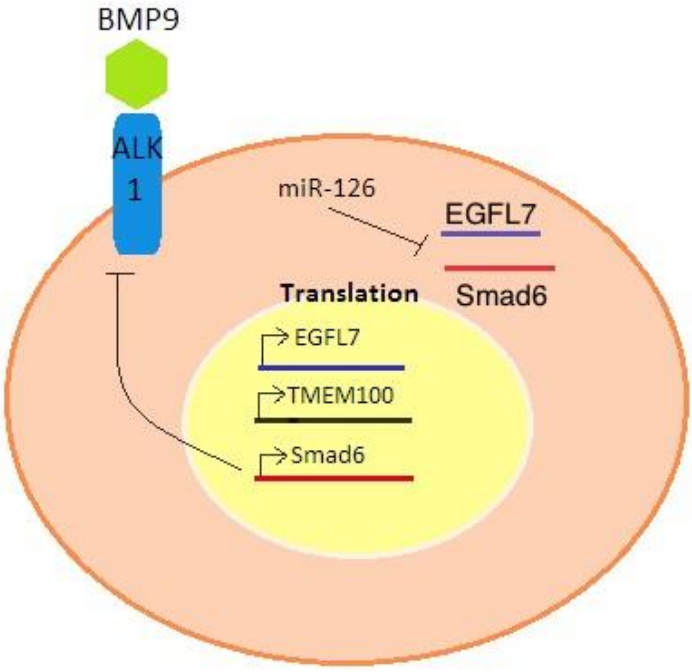

Figure 15. Common regulatory pathway. Illustration of how EGFL7, TMEM100, Smad6 and miR-126 could function together in one pathway to regulate endothelial development.

The results of this study provide one example of how miR-126 can affect endothelial development. Previous studies have however already illustrated an important role for miR-126 in angiogenesis. Research has shown that miR-126 regulates the endothelial cell response to VEGF during angiogenesis by repressing SPRED1, a negative regulator of the VEGF pathway (Nikolic et al. 2010). Furthermore, miR-126 mediated repression of SPRED1 has been shown to promote cell proliferation, migration and inhibit apoptosis in endothelial progenitor cells, whereas miR-126 knockdown and subsequent up-regulation of SPRED1 inhibits cell proliferation, migration and promotes apoptosis (Meng et al. 2012).

As previously mentioned, the exact role of EGFL7 and Smad6 in endothelial development is still unclear. The first definite evidence that EGFL7 played an important part in vascular development came from a study on tube formation in zebrafish that had an EGFL7 deletion. The zebrafish had an impaired cord-to-tube transition and this led to the formation of vessels with severely disorganized lumens or none at all. More specifically, cell migration of the angioblasts was impaired and they retained cell junctions (Nikolic et al. 2010). Because miR-126 has been shown to promote cell migration through down-regulation of SPRED1 and this study illustrated that miR-126 can also target EGFL7 and Smad6 it would be interesting to research whether there is a connection between these two pathways.

5.2 Concluding remarks

I have shown that miR-126 can bind the 3'UTR sequence of EGFL7 and Smad6 but not TMEM100. These results provide an example of how the TGFβ signaling pathway, EGFL7 and miR-126 could function together to regulate endothelial development. Even though this study has shown that EGFL7 and Smad6 are targets of miR-126, further research is needed to illustrate how miR-126 affects expression of these two genes. Furthermore, more research on whether EGFL7, Smad6, TMEM100 and miR-126 could all function together in one pathway during endothelial development is still needed

6 Bibliography

Bertolino, P. et al., 2005. Transforming growth factor-beta signal transduction in angiogenesis and vascular disorders. *Chest*, 128(6 Suppl), p.585S–590S. Available at: http://www.ncbi.nlm.nih.gov/pubmed/16373850 [Accessed April 2, 2015].

Bray, S.J., 2006. Notch signalling: a simple pathway becomes complex. *Nature reviews. Molecular cell biology*, 7(9), pp.678–89. Available at: http://dx.doi.org/10.1038 /nrm2009 [Accessed July 11, 2014].

Brennecke, J. et al., 2005. Principles of microRNA-target recognition. *PLoS biology*, 3(3), p.e85. Available at: http://www.pubmedcentral.nih.gov/articler ender.fcgi? artid=1043860&tool=pmcentrez&rendertype=abstract [Accessed July 10, 2014].

Burdick, J.A. & Vunjak-Novakovic, G., 2009. Engineered microenvironments for controlled stem cell differentiation. *Tissue engineering. Part A*, 15(2), pp.205–19. Available at: http://www.pubmedcentral.nih.gov/articlerender.fcgi?artid=2716398& tool=pmcentrez&rendertype=abstract [Accessed March 20, 2015].

Carmeliet, P. & Jain, R.K., 2011. Molecular mechanisms and clinical applications of angiogenesis. *Nature*, 473(7347), pp.298–307. Available at: http://www.pubmedcent ral.nih.gov/articlerender.fcgi?artid=4049445&tool=pmcentrez&rendertype=abstract [Accessed July 9, 2014].

Van Cruijsen, H., Giaccone, G. & Hoekman, K., 2005. Epidermal growth factor receptor and angiogenesis: Opportunities for combined anticancer strategies. *International journal of cancer. Journal international du cancer*, 117(6), pp.883–8. Available at: http://www.ncbi.nlm.nih.gov/pubmed/16152621 [Accessed March 24, 2015].

Developmental Biology, Ninth Edition. (2010) (p. 711). Sinauer Associates, Inc.; Ninth edition. Retrieved from http://www.amazon.com/Developmental-Biology-Ninth-Edition/dp/0878933840/ref=sr_1_2?ie=UTF8&qid=1397486902&sr=8-2&keywords=developmental+biology

Doss, M.X. et al., 2012. Specific gene signatures and pathways in mesodermal cells and their derivatives derived from embryonic stem cells. *Stem cell reviews*, 8(1), pp.43–54. Available at: http://www.ncbi.nlm.nih.gov/pubmed/21519850 [Accessed March 24, 2015].

Drake, C.J., 2003. Embryonic and adult vasculogenesis. *Birth defects research. Part C, Embryo today : reviews*, 69(1), pp.73–82. Available at: http://www.ncbi.nlm.nih.gov/ pubmed/12768659 [Accessed March 24, 2015].

Du, T. & Zamore, P.D., 2005. microPrimer: the biogenesis and function of microRNA. *Development (Cambridge, England)*, 132(21), pp.4645–52. Available at: http://dev.biologists.org/content/132/21/4645.long [Accessed March 19, 2015].

Fabian, M.R., Sonenberg, N. & Filipowicz, W., 2010. Regulation of mRNA translation and stability by microRNAs. *Annual review of biochemistry*, 79, pp.351–79. Available at: http://www.ncbi.nlm.nih.gov/pubmed/20533884 [Accessed July 14, 2014].

Filipowicz, W., Bhattacharyya, S.N. & Sonenberg, N., 2008. Mechanisms of post-transcriptional regulation by microRNAs: are the answers in sight? *Nature reviews. Genetics*, 9(2), pp.102–14. Available at: http://www.ncbi.nlm.nih.gov/ pubmed/ 18197166 [Accessed July 10, 2014].

Fish, J.E. et al., 2008. miR-126 regulates angiogenic signaling and vascular integrity. *Developmental cell*, 15(2), pp.272–84. Available at: http://www.pubmed cen tral. nih.gov/articlerender.fcgi?artid=2604134&tool=pmcentrez&rendertype=abstract [Accessed March 1, 2015].

Hata, A. et al., 1998. Smad6 inhibits BMP/Smad1 signaling by specifically competing with the Smad4 tumor suppressor. *Genes & Development*, 12(2), pp.186–197. Available at: http://genesdev.cshlp.org/content/12/2/186.long [Accessed April 2, 2015].

Heo, J. et al., 2005. Spontaneous differentiation of mouse embryonic stem cells in vitro: characterization by global gene expression profiles. *Biochemical and biophysical research communications*, 332(4), pp.1061–9. Available at: http://www.science direct.com/science/article/pii/S0006291X05009666 [Accessed March 23, 2015].

Jones-Rhoades, M.W., Bartel, D.P. & Bartel, B., 2006. MicroRNAS and their regulatory roles in plants. *Annual review of plant biology*, 57, pp.19–53. Available at: http://www.ncbi.nlm.nih.gov/pubmed/16669754 [Accessed July 9, 2014].

Larrivée, B. et al., 2012. ALK1 signaling inhibits angiogenesis by cooperating with the Notch pathway. *Developmental cell*, 22(3), pp.489–500. Available at: http://www.scien cedirect.com/science/article/pii/S153458071200086X [Accessed April 2, 2015].

Meng, S. et al., 2012. Downregulation of microRNA-126 in endothelial progenitor cells from diabetes patients, impairs their functional properties, via target gene Spred-1. *Journal of molecular and cellular cardiology*, 53(1), pp.64–72. Available at: http://www.ncbi.nlm.nih.gov/pubmed/22525256 [Accessed May 10, 2015].

Mirella Meregalli, A.F. and Y.T., 2011. *Stem Cells in Clinic and Research* A. Gholamrezane-zhad, ed., InTech. Available at: http://www.intechopen.com/books/ stem-cells-in-clinic-and-research/stem-cell-therapy-for-neuromuscular-diseases [Accessed April 19, 2015].

Moser, M. & Patterson, C., 2005. Bone morphogenetic proteins and vascular differentiation: BMPing up vasculogenesis. *Thrombosis and haemostasis*, 94(4), pp.713–8. Available at: http://www.ncbi.nlm.nih.gov/pubmed/16270622 [Accessed March 24, 2015].

Nichol, D. & Stuhlmann, H., 2012. EGFL7: a unique angiogenic signaling factor in vascular development and disease. *Blood*, 119(6), pp.1345–52. Available at: http://www.pubmedcentral.nih.gov/articlerender.fcgi?artid=3286203&tool=pmcent rez&rendertype=abstract [Accessed April 1, 2015].

Nikolic, I., Plate, K.-H. & Schmidt, M.H., 2010. EGFL7 meets miRNA-126: an angiogenesis alliance. *Journal of Angiogenesis Research*, 2(1), p.9. Available at: http://www.pubmedcentral.nih.gov/articlerender.fcgi?artid=2901201&tool=pmcentrez&rendertype=abstract [Accessed March 20, 2015].

Otrock, Z.K. et al., Understanding the biology of angiogenesis: review of the most important molecular mechanisms. *Blood cells, molecules & diseases*, 39(2), pp.212–20. Available at: http://www.ncbi.nlm.nih.gov/pubmed/17553709 [Accessed February 24, 2015].

Parker, L.H. et al., 2004. The endothelial-cell-derived secreted factor Egfl7 regulates vascular tube formation. *Nature*, 428(6984), pp.754–8. Available at: http://www.ncbi.nlm.nih.gov/pubmed/15085134 [Accessed March 27, 2015].

Passier, R. & Mummery, C., 2003. Origin and use of embryonic and adult stem cells in differentiation and tissue repair. *Cardiovascular research*, 58(2), pp.324–35. Available at: http://www.ncbi.nlm.nih.gov/pubmed/12757867 [Accessed March 23, 2015].

Puri, M.C. & Nagy, A., 2012. Concise review: Embryonic stem cells versus induced pluripotent stem cells: the game is on. *Stem cells (Dayton, Ohio)*, 30(1), pp.10–4. Available at: http://www.ncbi.nlm.nih.gov/pubmed/22102565 [Accessed March 20, 2015].

Ratajczak, M.Z. et al., 2008. Hunt for pluripotent stem cell -- regenerative medicine search for almighty cell. *Journal of autoimmunity*, 30(3), pp.151–62. Available at: http://www.pubmedcentral.nih.gov/articlerender.fcgi?artid=2692479&tool=pmcentrez&rendertype=abstract [Accessed February 17, 2015].

Risau, W. & Flamme, I., 1995. Vasculogenesis. *Annual review of cell and developmental biology*, 11, pp.73–91. Available at: http://www.ncbi.nlm.nih.gov/ pubmed/ 8689573 [Accessed March 24, 2015].

Scharpfenecker, M. et al., 2007. BMP-9 signals via ALK1 and inhibits bFGF-induced endothelial cell proliferation and VEGF-stimulated angiogenesis. *Journal of cell science*, 120(Pt 6), pp.964–72. Available at: http://www.ncbi.nlm.nih.gov/pubmed/17311849 [Accessed May 8, 2015].

Schmidt, M.H.H. et al., 2009. Epidermal growth factor-like domain 7 (EGFL7) modulates Notch signalling and affects neural stem cell renewal. *Nature cell biology*, 11(7), pp.873–80. Available at: http://www.ncbi.nlm.nih.gov/pubmed/ 19503073 [Accessed April 1, 2015].

Shahriyari, L. & Komarova, N.L., 2013. Symmetric vs. asymmetric stem cell divisions: an adaptation against cancer? *PloS one*, 8(10), p.e76195. Available at: http://www.pubmedcentral.nih.gov/articlerender.fcgi?artid=3812169&tool=pmcentrez&rendertype=abstract [Accessed January 21, 2015].

Shu, J. et al., 2012. Dose-dependent differential mRNA target selection and regulation by let-7a-7f and miR-17-92 cluster microRNAs. *RNA biology*, 9(10), pp.1275–87. Available at: http://www.pubmedcentral.nih.gov/articlerender.fcgi? artid=3583858 & tool=pmcentrez&rendertype=abstract [Accessed May 10, 2015].

Somekawa, S. et al., 2012. Tmem100, an ALK1 receptor signaling-dependent gene essential for arterial endothelium differentiation and vascular morphogenesis. *Proceedings of the National Academy of Sciences of the United States of America*, 109(30), pp.12064–9. Available at: http://www.pubmedcentral.nih.gov/ articler ender.fcgi? artid= 3409742 &tool=pmcentrez&rendertype=abstract [Accessed March 20, 2015].

Sontheimer, E.J., 2005. Assembly and function of RNA silencing complexes. *Nature reviews. Molecular cell biology*, 6(2), pp.127–38. Available at: http://www.ncbi.nlm. nih.gov/ pubmed/15654322 [Accessed May 6, 2015].

Suzuki, Y. et al., 2010. BMP-9 induces proliferation of multiple types of endothelial cells in vitro and in vivo. *Journal of cell science*, 123(Pt 10), pp.1684–92. Available at: http://www.ncbi.nlm.nih.gov/pubmed/20406889 [Accessed April 2, 2015].

Vasudevan, S., Posttranscriptional upregulation by microRNAs. *Wiley interdisciplinary reviews. RNA*, 3(3), pp.311–30. Available at: http://www.ncbi.nlm.nih.gov/pubmed/ 22072587 [Accessed April 15, 2015].

Velazquez, O.C., 2007. Angiogenesis and vasculogenesis: inducing the growth of new blood vessels and wound healing by stimulation of bone marrow-derived progenitor cell mobilization and homing. *Journal of vascular surgery*, 45 Suppl A, pp.A39–47. Available at: http://www.pubmedcentral.nih.gov/articlerender.fcgi? artid= 2706093&tool=pmcentrez&rendertype=abstract [Accessed March 24, 2015].

Wang, S. et al., 2008. The endothelial-specific microRNA miR-126 governs vascular integrity and angiogenesis. *Developmental cell*, 15(2), pp.261–71. Available at: http://www.pubmedcentral.nih.gov/articlerender.fcgi?artid=2685763&tool=pmcent rez&rendertype=abstract [Accessed October 14, 2014].

Welti, J. et al., 2013. Recent molecular discoveries in angiogenesis and antiangiogenic therapies in cancer. *The Journal of clinical investigation*, 123(8), pp.3190–200. Available at: http://www.pubmedcentral.nih.gov/articlerender.fcgi?artid= 3726176 &tool=pmcentrez&rendertype=abstract [Accessed May 6, 2015].

Wu, L., Fan, J. & Belasco, J.G., 2006. MicroRNAs direct rapid deadenylation of mRNA. *Proceedings of the National Academy of Sciences of the United States of America*, 103(11), pp.4034–9. Available at: http://www.pubmedcentral.nih.gov/article render. fcgi? artid =1449641&tool=pmcentrez&rendertype=abstract [Accessed May 6, 2015].

Yin, T. & Li, L., 2006. The stem cell niches in bone. *The Journal of clinical investigation*, 116(5), pp.1195–201. Available at: http://www.pubmedcentral.nih.gov/ article render.fcgi?artid=1451221&tool=pmcentrez&rendertype=abstract [Accessed March 23, 2015].

Zhang, Y. et al., 2013. miR-126 and miR-126* repress recruitment of mesenchymal stem cells and inflammatory monocytes to inhibit breast cancer metastasis. *Nature cell biology*, 15(3), pp.284–94. Available at: http://dx.doi.org/10.1038/ncb2690 [Accessed May 10, 2015].

7 Appendix A

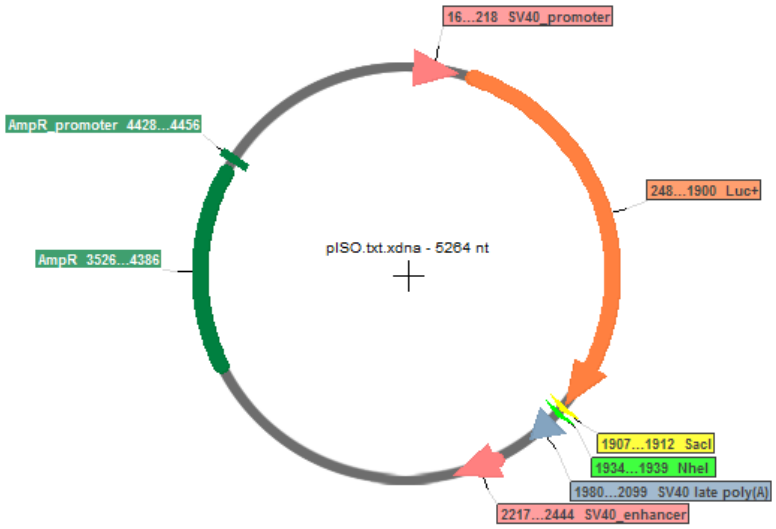

Figure A1. Graphic map of pISO plasmid.

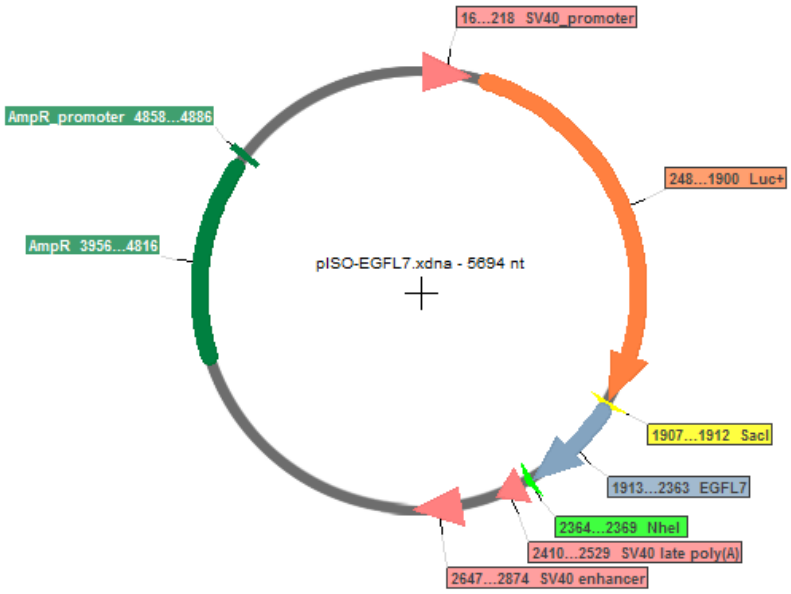

Figure A2. Graphic map of pISO plasmid with 3'UTR EGFL7 insert.

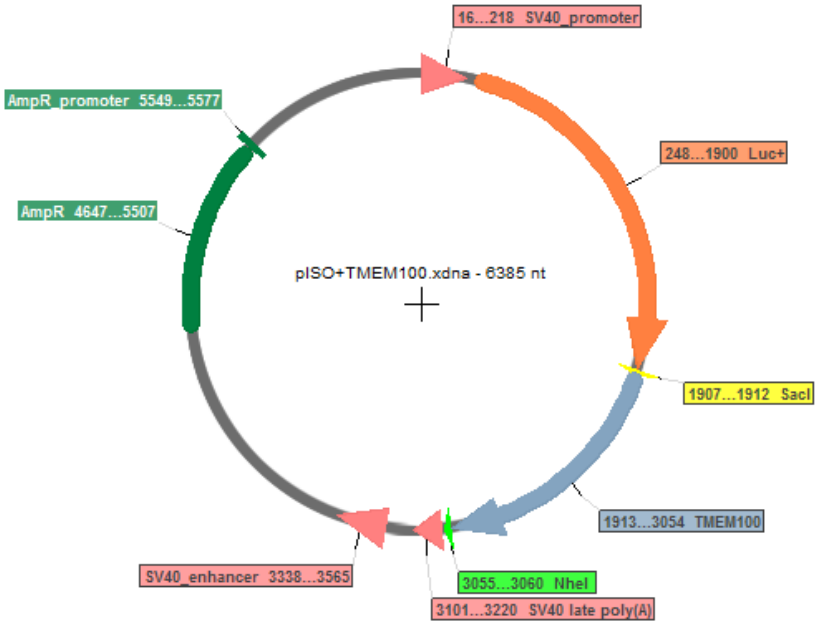

Figure A3. Graphic map of pISO plasmid with 3'UTR TMEM100 insert.

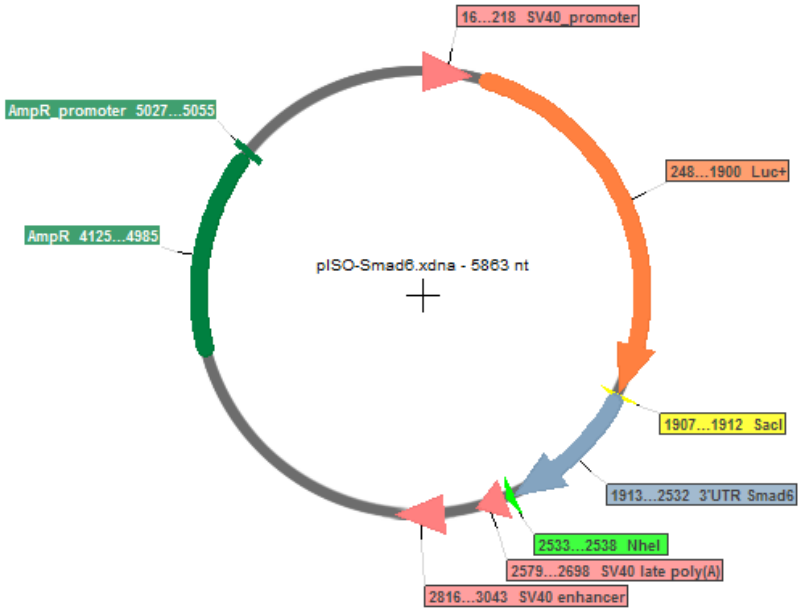

Figure A4. Graphic map of pISO plasmid with 3'UTR Smad6 insert.

8 Appendix B

5’
CCTCCTCAACAACCCCAGATAGTGGCGGCCCCGGCGGGAGGGGCGGGTGGG
AGGCCGCGGCCACCGCCACCTGCCGGCCTCGAGAGGGGCCGATGCCCAGAG
ACACAGCCCCCACGGACAAAACCCCCCAGATATCATCTACCTAGATTTAATA
TAAAGTTTTATATATTATATGGAAATATATATTATACTTGTAATTATGGAGTC
ATTTTTACAATGTAATTATTTATGTATGGTGCAATGTGTGTATATGGACAAA
ACAAGAAAGACGCACTTTGGCTTATAATTCTTTCAATACAGATATATTTTCTT
TCTCTTCCTCCTTCCTCTTCCTTACTTTTTATATATATATATATAAAGAAAATGAT
ACAGCAGAGCTAGGTGGAAAAGCCTGGGTTTGGTGTATGGTTTTTGAGATAT
TAATGCCCAGACAAAAAGCTAATACCAGTCACTCGATAATAAAGTATTCGC
ATTATAGTTTTTTTTAAACTGTCTTCTTTTTACAAAGAGGGGCAGGTAGGGCT
TCAGCGGATTTCTGACCCATCATGTACCTTGAAACTTGACCTCAGTTTTCAAG
TTTTACTTTTATTGGATAAAGACAGAACAAATTGAAAAGGGAGGA **3’**

Figure B1: 3’UTR Smad 6 insert.

5’
AAGAAAGCCAAGAGACGGGAGAGTCAAACAGCTCTCGTGGCAAATCAGAG
AAGCTTGTTTGCTTGAGACTGAATACGACCAAATGGGCCATTGGGCCTGGAA
AACGTGCTCTGACTTTGTCACCCAATTCACCCAGAACCATGGTGGGAGAGAA
CAGACTTGGCGTTGGAGCAGACTGGAAGAATGGGGGTGGGAGGGTGGAGG
GGCTTCTCCTTTGTGAGGAATGACTCATGTCTTCTTTAACGACAAACTTAACC
CTAAGGGCTACTTCTGAGACTGAAAAATCAGCTTTCTATTTACATGAAACAC
TTTGGGGGTCATGGGAGTGCACAGCATTAGACAGTATTTGGTTCACCCTGTA
AAGTAGCCAAGAAAAGATGAGAAAAATCAAGATAGGCCTGGCACACTAGA
CATTTGCCTCCAAAAGAAATAACCTACAGTCTTAAGATGTATCATAAAAATG
TTCTGCCAAGGATCTAAATTACCTTGGGTTTCGCATATGTCTATGAAATTCTG
TGATAATTTTTTTCAATACATTGATTCACTGGCGTCTGTTTTCATTTTATACTT
TTAATAACTCATCACTGGTGGTACTTTATCTTGAAAAGTAATATTTTTTATAT
TTTAACATTGGACAGTGTTAGCCAGTTGTAATGATGTATCAGAAGTAAAGAA
AAACCCATTAAAGTTATAGCTAATAGATGCTGTTGGGGGTTAAATTAATAGT
AAAATAATCCAATATAGCACTTTTGATGATTTTTATATAAAAGTCAACTGTA
CATTTCATTCAGAATAATAAATACTTATTGCTGCTAAAACTTCTTAAATGGTT
GTTTCTGCTATAGTTATTTCTATTGCAGTTCCAAATTGCCATCTTCCCTTGTCT
CATTTGCAAGTTCTCAATTGTATTTCTCTCAAATGGACAGGTTCCTTCTTTAC
TGGAGGATTTTTGTTTTTATCATATTGGTTTTTCATTACTTCTGAATAGTCTTA
ATTACGTTTACTAAATTCTAAAGGATTTCTGTGCTATTATAATTAGGAAATCA
ACGTCTTTGGTCAGGAACTTTATAATGTGCTATTAAATGTATATTACATTTTT
GTGGAATCAGTTGTTAATTATTTGCTTAACACGTATGCCAGCA **3’**

Figure B2: 3’UTR TMEM100 insert.